Work Order No. 582-23-45978-014
Contract No. 582-23-45978
Tracking No. 2025-15
Task 4.1

Prepared for:

Texas Commission on Environmental Quality
12100 Park 35 Circle MC 164
Austin, TX 78753

Prepared by:

Ramboll
7250 Redwood Blvd., Suite 105
Novato, California 94945

July 2025

September 2019/2023 Modeling Intercomparison

PREPARED UNDER A CONTRACT FROM THE
TEXAS COMMISSION ON ENVIRONMENTAL QUALITY

The preparation of this document was financed through a contract from the State of Texas through the Texas Commission on Environmental Quality.
The content, findings, opinions and conclusions are the work of the author(s) and do not necessarily represent findings, opinions or conclusions of the TCEQ.

RAMBOLL

September 2019/2023 Modeling Intercomparison

Final Report

Ramboll
7250 Redwood Boulevard
Suite 105
Novato, CA 94945
USA

T +1 415 899 0700
https://ramboll.com

Contents

Appendix

Figures

Tables

LIST OF ACRONYMS AND ABBREVIATIONS

AQS	Air Quality System
BC	Boundary Condition
CAMx	Comprehensive Air Quality Model with Extensions
DFW	Dallas Fort-Worth
EGU	electrical generating unit
EI	emissions inventory
hPa	hectopascal
HGB	Houston-Galveston-Brazoria
Mb	millibars
MDA8	daily maximum 8-hr average ozone
NAA	non-attainment area
NAAQS	national ambient air quality standard
NCEP	National Centers for Environmental Prediction
NMB	normalized mean bias
NME	normalized mean error
NOAA	National Oceanic and Atmospheric Administration
NO_X	nitrogen dioxides
OSAT	ozone source apportionment technology
PBL	planetary boundary layer
Ppb	parts per billion
PSL	Physical Sciences Laboratory
Q-Q	quantile – quantile
R	correlation coefficient
SIPs	State Implementation Plans
TCEQ	Texas Commission on Environmental Quality
VOC	Volatile Organic Compounds
WRF	weather research forecast

PROJECT SUMMARY

The purpose of this work was to better understand the conditions that contributed to high ozone observed in Texas in September 2023 and to identify factors that explain why attainment demonstration modeling based on 2019 showed lower projected modeled ozone in 2023 than was observed. This work provides insights into the various model inputs that drive differences between 2023 modeled and observed ozone concentrations, which could inform the development of TCEQ's 2022 modeling platform.

EXECUTIVE SUMMARY

The TCEQ has found that model-projected 2023 attainment year ozone concentrations based on 2023 emissions and 2019 base year meteorology were substantially lower than observed conditions in 2023. This project investigated the causes of the 2023 underpredictions by contrasting those ozone predictions with two additional model scenarios: (1) using 2023 meteorology, and (2) using updated 2023 emissions and model boundary conditions, to quantitatively characterize the roles of meteorology and emissions in influencing high ozone in September 2023.

Ramboll quantitatively compared model inputs (i.e., meteorology) and model outputs (i.e. total ozone concentrations and ozone contributions from tracked emission source groups and boundary contributions) for the three scenarios simulated by the Comprehensive Air quality Model with extensions (CAMx). Comparisons were conducted for all Texas ozone nonattainment areas (NAA) within the 4 km Texas modeling domain. Ramboll compared ozone concentration distributions among observed and simulated maximum daily 8-hour (MDA8) ozone concentrations. Furthermore, Ramboll compared meteorological parameters simulated by the Weather Research and Forecasting model (WRF) during September 2019 and September 2023, such as temperature, winds, humidity, cloud cover, and planetary boundary layer (PBL) depth.

The primary reason that the attainment demonstration modeling projected lower modeled ozone than observed was that it was based on 2019 meteorology, which was less conducive to ozone formation than 2023. Meteorological conditions in September 2023 were more conducive to ozone formation since that period was characterized by more stagnant winds and much less southerly flow (i.e., less transport of cleaner air from the Gulf of Mexico), as well as warmer temperatures and sunnier skies. Updating the modeling to 2023 meteorology and updating 2023 emissions resulted in higher modeled ozone concentrations and improved model performance compared to the attainment demonstration modeling but still underestimated peak ozone. There were mixed changes due to updating the boundary conditions.

Running CAMx with updated 2023 emissions (i.e., as well as updated 2023 meteorology) simulated lower total MDA8 ozone than using updated 2023 meteorology alone. Ozone source apportionment technology (OSAT) revealed that using 2023 fires instead of 2019 fires resulted in the largest ozone reductions of all tracked sectors; thus, 2019 fire emissions offset model underestimates in 2023. This is often termed "getting the right answer for the wrong reason". Contributions from electric generating units (EGU) were marginally impactful.

Ramboll recommends further study to investigate additional reasons for the ongoing underestimates. Key to this would be to update other major source categories like mobile source emissions. Furthermore, WRF meteorological model performance for wind speeds

should be investigated, since the analyses suggest wind speeds are overestimated and could lead to underestimates of ozone due to increased ventilation of local emissions.

1.0 INTRODUCTION

1.1 Background

The TCEQ developed a 2019 modeling platform, based on the Comprehensive Air quality Model with extensions (CAMx; Ramboll, 2024), to support the latest round of ozone State Implementation Plan (SIP) revisions for Texas ozone nonattainment areas. The 2019 platform exhibited some model performance issues in replicating observed conditions. Furthermore, simulated 2023 attainment year ozone concentrations based on 2023 emissions projected from the 2019 base year were substantially lower than observed conditions in 2023. This project investigated the causes of the 2023 underpredictions (focused on September) by contrasting those ozone predictions with two additional model scenarios: (1) using 2023 meteorology, and (2) using updated 2023 emissions and model boundary conditions, to quantitatively characterize the roles of meteorology and emissions in influencing high ozone in September 2023.

1.2 Approach

Ramboll quantitatively compared CAMx model inputs (i.e., meteorology) and CAMx model outputs (i.e. total ozone concentrations and ozone contributions from tracked emission source groups and boundary contributions), for the three scenarios listed below. Comparisons were conducted for all Texas ozone nonattainment areas within the 4 km Texas modeling domain as shown in Figure 1-1. Ramboll compared ozone concentration distributions among observed and simulated maximum daily 8-hour (MDA8) ozone concentrations. Furthermore, Ramboll compared meteorological parameters simulated by the Weather Research and Forecasting model (WRF; Skamarock, 2019) during September 2019 and September 2023, such as temperature, winds, humidity, cloud cover, and planetary boundary layer (PBL) depth.

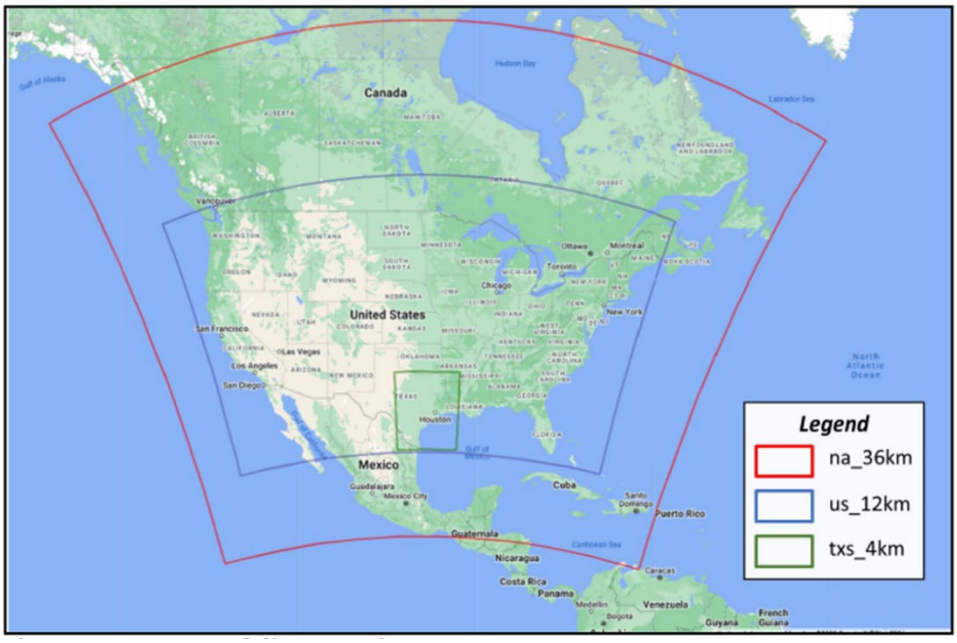

Figure 1-1. CAMx nested 36 km, 12 km and 4 km modeling grids.

1.3 Model Scenarios

The following modeling scenarios were evaluated:

1) **Run 1 - 2019 modeling platform:** September 2019 meteorological inputs, 2023 future year (FY) emission projections from the 2019 modeling platform, simulated total ozone from the 2023 FY scenario, and ozone contributions from emissions and boundary conditions from the FY2023 scenario.

2) **Run 2 - 2023 meteorology:** As in (1), except 2023 simulated meteorology replaced 2019 meteorology.

3) **Run 3 - 2023 modeling platform:** As in (2), except updated 2023 emissions inventory (EI) for year-specific emission sectors replaced the projected FY2023 EI (biogenics, fires, Texas and non-Texas electrical generating units [EGUs], and other non-EGU point sources). Also, 2023-specific boundary conditions replaced the FY2023 boundary conditions.

All three CAMx runs were completed by TCEQ, and the outputs were provided to Ramboll.

1.4 Monitor Selection

The focus of this study was to evaluate CAMx model predictions in the three Texas ozone nonattainment areas (NAA) that are located within the 4 km Texas modeling domain (i.e., Dallas-Fort Worth (DFW), San Antonio, and Houston-Galveston-Brazoria (HGB)). Figure 1-2 provides a map of Texas ozone NAAs. For each NAA, Ramboll designated the monitor with the highest 2021-2023 ozone design values (DV) as the primary monitor. The primary monitors, the corresponding Air Quality System (AQS) codes, and design values are listed in Table 1-1.[1] Additional monitors that are used for intra-NAA analyses are described below.

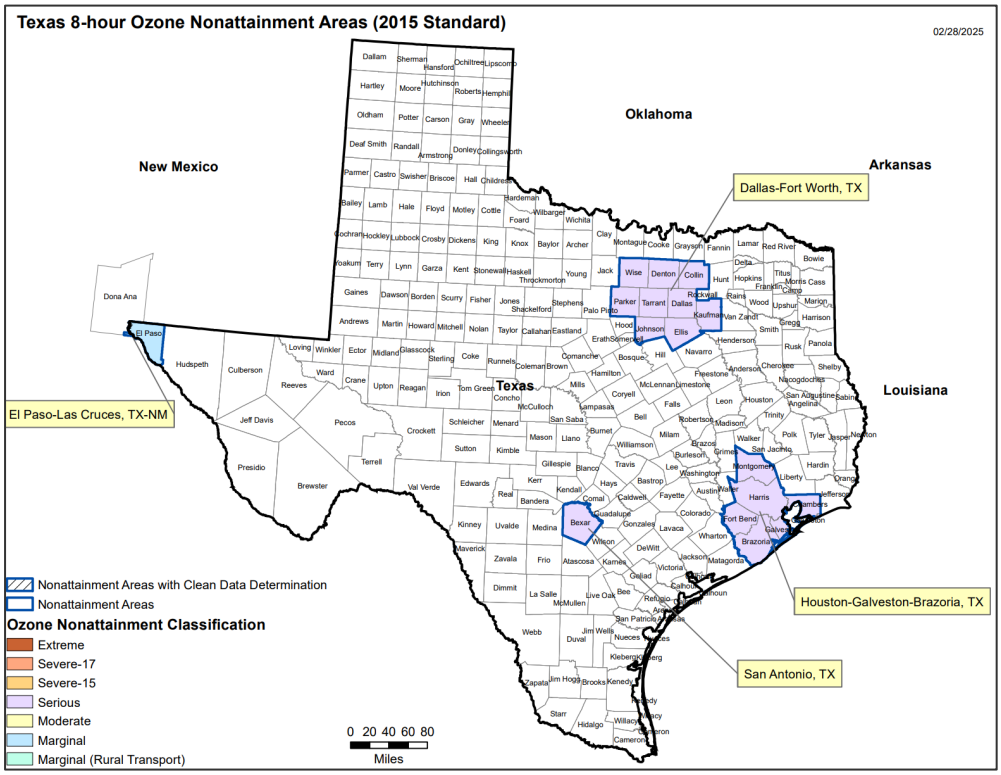

Figure 1-2. Texas 8-hour ozone nonattainment areas (2015 NAAQS), showing the 3 serious NAAs evaluated in this study.[2]

[1] The ozone design value is the 3-year average of the annual fourth-highest daily maximum 8-hour average ozone concentration, used to determine if an area meets the National Ambient Air Quality Standards (NAAQS).

[2] https://www3.epa.gov/airquality/greenbook/map/tx8_2015.pdf

Table 1-1. Primary monitors selected for the analysis.

Nonattainment Area	Primary Monitor	AQS Site ID	2021-2023 ozone DV
Houston-Galveston-Brazoria (HGB)	Bayland Park	482010055	83 ppb
Dallas-Fort Worth (DFW)	Pilot Point	481211032	81 ppb
San Antonio	Camp Bullis	480290052	76 ppb

1.4.1 Intra-NAA Analyses

To evaluate variations within each NAA, additional monitors were selected based on discussions with TCEQ (Table 1-2). All ozone analyses that are presented for the primary monitors are also presented for the additional monitors in Appendix A. A comparison of total ozone within each NAA is provided as quantile-quantile (Q-Q) plots in the main body of this report.

Table 1-2. Intra-NAA monitors selected for the analysis.

Nonattainment Area	Additional Selected Monitor(s)	AQS Site ID	2021-2023 ozone DV
HGB	Clinton	482011035	76 ppb
HGB	Aldine	482010024	72 ppb
HGB	Conroe Relocated	483390078	71 ppb
DFW	Kaufman	482570005	67 ppb
DFW	Fort Worth Northwest	484391002	80 ppb
San Antonio	Calaveras Lake	480290059	69 ppb

2.0 OZONE COMPARISON

All ozone analyses are presented in terms of MDA8 ozone concentrations, the standard metric for the ozone NAAQS. Ramboll extracted CAMx model output data for the grid cells that correspond to the selected monitors. Spatial details of the primary monitors are presented in Table 2-1. Spatial details of the additional monitors are presented in Appendix A.

Table 2-1. Spatial details of primary monitors.

Monitor	AQS#	Latitude	Longitude	CAMx 4km grid I	CAMx 4km grid J
Bayland Park (HGB)	482010055	29.6957º	-95.4992º	118	111
Pilot point (DFW)	481211032	33.4106º	-96.9446º	83	214
Camp Bullis (San Antonio)	480290052	29.6321º	-98.5649º	43	109

2.1 Total Ozone

The total ozone analysis compared modeled CAMx output from Run 1, Run 2, and Run 3 with observed ozone concentrations in terms of timeseries plots and quantile-quantile (Q-Q) plots. Timeseries plots are intuitive but have limitations for this analysis since there is a mismatch in meteorological years for Run 1 when compared with 2023 observed ozone, and therefore a temporal agreement is not expected. For that reason, Q-Q plots are also presented, which facilitate comparison between the distributions of data that are unmatched in time and are more appropriate for this analysis. Normalized mean bias (NMB), normalized mean error (NME) and the correlation coefficient (R) are also reported based on MDA8 ozone, which are standard performance metrics to quantitatively evaluate model performance (Emery et.al., 2017).

2.2 OSAT Emissions Source Group Contributions

The OSAT analyses examined source contributions from boundary conditions (stratified by the four lateral domain edges) as well as source contributions from fires, biogenic sources and all anthropogenic sources. Note that the Boundary Condition (BC) impacts refer to contributions from all natural and anthropogenic sources outside the 36 km CAMx grid as shown in Figure 1-1. Sources were tracked within the CAMx Ozone Source Apportionment Technology (OSAT) probing tool. The OSAT tracers and descriptions are presented in Table 2-2. Note that "O3N" refers to ozone that is formed under NO_X-limited conditions and there is an equivalent set of OSAT tracers for VOC-limited conditions (O3V). NO_X-limited and VOC-limited ozone contributions are summed in the following analyses.

Table 2-2. CAMx OSAT emission source groups.

OSAT Tracers	Description
O3N000IC	Initial Condition
O3NWSTBC	West BC
O3NESTBC	East BC
O3NSTHBC	South BC
O3NNTHBC	North BC
O3NTOPBC	Top BC
O3N001001	Biogenic
O3N002001	Fire
O3N003001	Texas EGU
O3N004001	Non-Texas EGU
O3N005001	Other anthropogenic

The OSAT analyses are presented in terms of Q-Q plots and compared emission source group contributions to MDA8 ozone for Run 1 compared to Run 2 and Run 2 compared to Run 3. Since the only difference between Run 1 and 2 is meteorology with no differences in emissions, the changes in the emission source contributions to MDA8 ozone were only driven by the different meteorology. There are two primary meteorologically driven causes for changing source contributions: (1) different atmospheric transport patterns among source regions reaching the impacted monitor (e.g., boundary condition contributions are highly impacted by transport patterns as well as contributions from other distant sources within the modeling domain), (2) ozone formation chemistry (e.g., warmer and sunnier days generally have higher photochemical ozone production). The difference between Run 2 and Run 3 is the change in emissions as described in Section 1.3.

A first set of OSAT Q-Q plots shows contributions from each of the boundary conditions, fires, biogenic sources and "All Anthropogenic" which is the sum of Texas EGU, non-Texas EGU and the other anthropogenic source groups. A second set of OSAT Q-Q plots retains the Texas EGU and non-Texas EGU as separate emissions source categories for comparing Run 2 and Run 3 (i.e., the runs that have differences in those emission source categories). Initial Conditions (i.e., model initial concentrations that tend to zero during the model spin-up period) and Top Conditions (i.e., from the model's top boundary concentrations) are omitted from the analysis since they are of negligible importance.

2.3 Houston

2.3.1 Total Ozone

presents a comparison of September MDA8 ozone for the three CAMx model runs against 2023 observed MDA8 ozone at the primary HGB monitor (Bayland Park). The Run 1 timeseries plot (upper left) shows different periods of relatively higher and lower MDA8 ozone, a consequence of comparing different meteorological years. The Run 1 Q-Q plot (upper right) shows consistent, substantial underpredicted ozone especially at the upper end of the range (i.e., above 60 ppb). This large underprediction was the impetus for this study. The Run 2 timeseries plot (middle left) shows much improved temporal agreement, resulting in better ozone alignment as shown in the timeseries and a substantial improvement in the Q-Q plot (middle right). Table 2-3 summarizes model performance statistics and shows that Run 2 MDA8 ozone better agrees with AQS observed MDA8 ozone than Run 1 both in terms of the September mean and 4th highest MDA8. In addition, the NMB, NME and R statistics are much improved for Run 2 compared to Run 1, since the negative bias is reduced substantially, the error is smaller, and the correlation (R) is much closer to one. (Note R = 1 is a perfect linear regression). The improvement of Run 2 performance compared to Run 1 performance was expected since Run 2 uses 2023 meteorology, which is consistent with the 2023 AQS data.

and Table 2-3 show a large improvement in the middle plot which suggests that meteorology played a substantial role in the Run 1 underpredictions. Differences in meteorological parameters between 2019 and 2023 are explored in Section 3.0.

The Run 3 timeseries is generally similar to the Run 2 timeseries with slightly lower peak values. At the higher end of the range (i.e., above 60 ppb), the Q-Q plot showed that Run 2 had the least severe underprediction followed by Run 3. The Table 2-3 statistics reflect this same phenomenon and report degraded model performance for Run 3 compared to Run 2 for NMB and NME. This result was not expected since the updated emissions in Run 3 were developed to provide a more accurate representation of meteorologically-driven emissions that theoretically should yield improved model performance. The following section explores differences in emission source group contributions to MDA8 ozone to better understand the impact of the different emissions in Run 2 versus Run 3.

Figure 2-1. CAMx ozone timeseries and Q-Q model performance comparisons at the primary Houston monitor.

Table 2-3. CAMx model performance summary statistics for the primary Houston area monitor (Bayland Park).

Metric	2023 AQS	Run 1	Run 2	Run 3
September Mean MDA8 [ppb]	59.9	48.1	57.0	53.5
September 4th high MDA8 [ppb]	85.0	65.1	75.5	72.1
NMB MDA8 %	-	-19.8	-5.0	-10.8
NME MDA8 %	-	37.8	11.0	14.2
R	-	-0.33	0.92	0.92

2.3.2 OSAT Emission Source Group Contributions

This section presents contributions to MDA8 ozone from different emission source groups at the Bayland Park, Houston monitor. The same analyses for the additional Houston monitors are provided in Appendix A.

Figure 2-2 shows Q-Q plots for CAMx OSAT source contributions to MDA8 ozone for Run 1 versus Run 2 (upper plot) and Run 2 versus Run 3 (lower plot). The "All Anthropogenic" source had the largest contribution for both meteorological years and both emissions scenarios and is approximately 10 - 15 ppb higher for Run 2 (i.e., with 2023 meteorology) than for Run 1 (i.e., with 2019 meteorology). This suggests that atmospheric transport pathways were more favorable for transport of emissions from that source category to the monitor and/or meteorological conditions were more favorable for ozone formation in 2023 compared to 2019. The difference in the "All Anthropogenic" source between Run 2 and Run 3 was relatively minimal compared to Run 1 versus Run 2. The biogenic contribution was greater for Run 2 as compared to Run 1 but comparable for Run 2 versus Run 3. All boundary condition contributions were generally lower for Run 2 than Run 1, in particular the eastern and northern boundaries. Western boundary conditions and fires had slightly lower contributions for Run 2 than Run 1. Differences in boundary condition impacts for Run 2 and Run 3 were minimal. The only substantial difference between Run 2 and Run 3 was for fires which had an approximately 2 to 7 ppb smaller contribution in Run 3 than Run 2.

Figure 2-3 provides a deeper exploration of the impact of the changes in emissions in Run 3 compared to Run 2. The boundary condition contributions were omitted, and Texas EGU and non-Texas EGU contributions are shown individually. Note that EGU emissions were adjusted in Run 3, and therefore it is important to evaluate the impact of those updated emissions. The upper and lower panels display the same data, but the lower panel "zooms in" on the smaller contributions to better discern the relatively smaller changes in the EGU contributions. Run 3 fire contributions are approximately one third of the contribution of Run 2 fire contributions, which equates to a reduction of approximately 2 - 4 ppb. This explains the lower total MDA8 ozone for Run 3 compared to Run 2, given that the other source contributions are similar (i.e., aligning along the 1:1 line). A spatial map of average fire impacts is provided in a subsequent section to provide a more complete understanding of the differences in fire contributions. Texas EGU and non-Texas EGU contributions ranged from 0 ppb to approximately 3 ppb. The non-Texas EGU impacts were generally slightly lower for Run 3 than Run 2 (by less than 0.5 ppb) and Texas EGU impacts were mixed with variations of less than 1 ppb in the positive and negative direction.

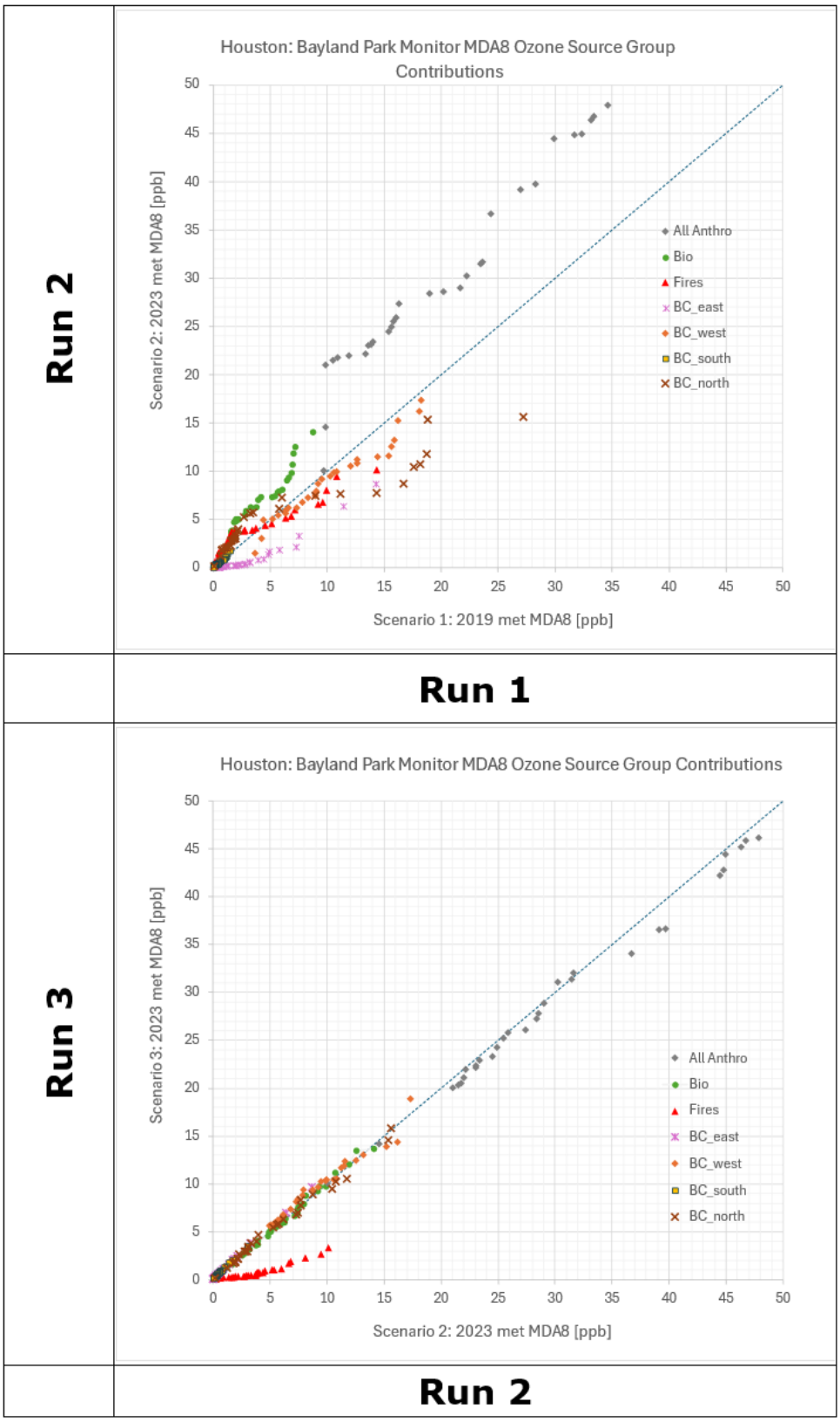

Figure 2-2. CAMx OSAT comparisons at Bayland Park, Houston NAA. Run 1 versus Run 2 and Run 2 versus Run 3.

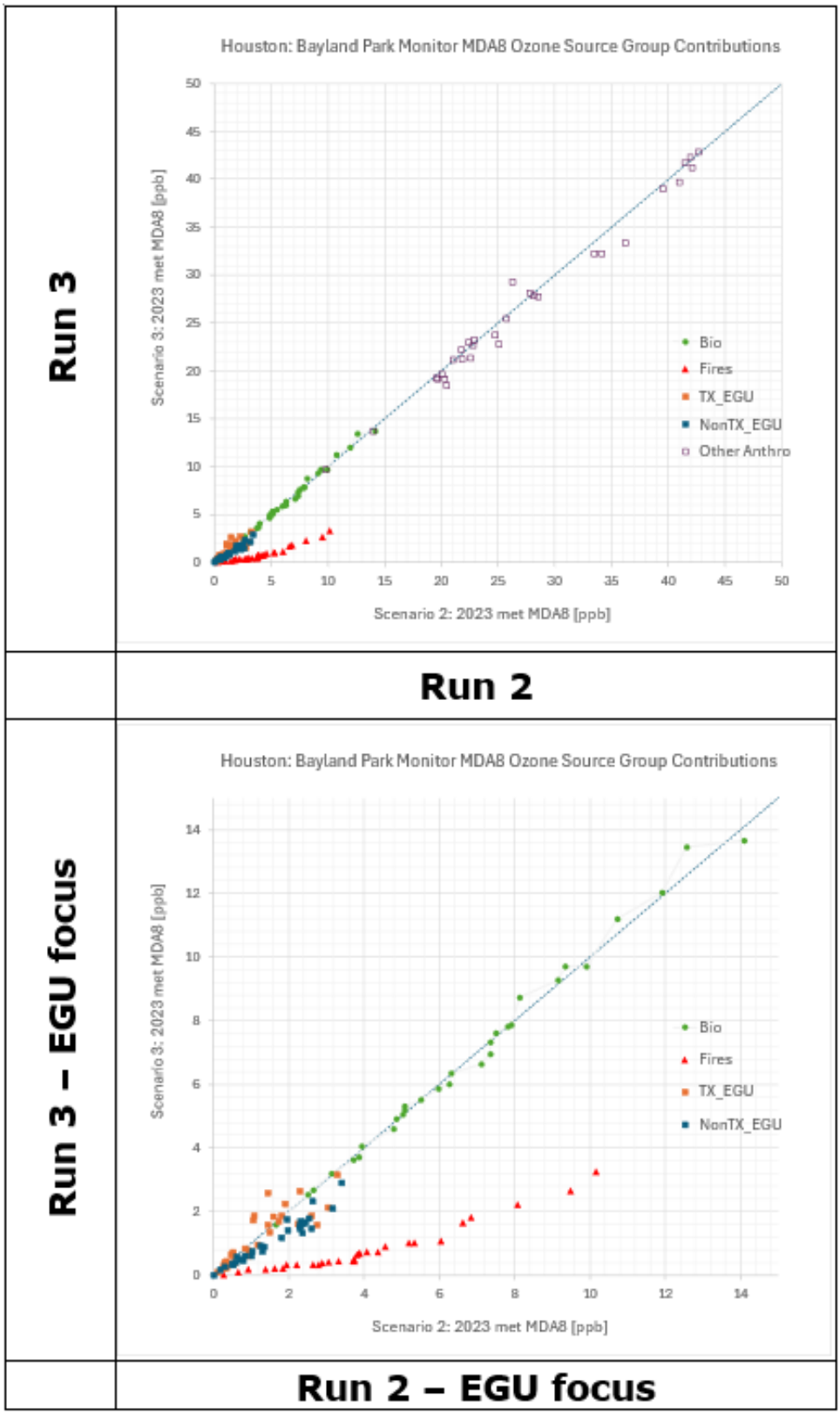

Figure 2-3. CAMx OSAT comparisons at Bayland Park, Houston NAA. Run 2 versus Run 3 with EGUs contributions separated.

2.3.3 Intra-Houston NAA

Appendix A reports the same analysis as shown above (i.e., for the primary Bayland Park, Houston NAA monitor) but for the 3 additional Houston NAA monitors.

Figure 2-4 compares total MDA8 ozone results for the 4 Houston monitors in terms of Q-Q plots. The Run 1 negative bias was most severe for Bayland Park and less so at the other locations in the Houston NAA, although Clinton also had a negative bias at the upper end of the distribution. Run 1 performed better at Aldine and Conroe except Aldine modeled 2 days with higher MDA8 ozone than was observed (Run 1 MDA8 > 80 ppb). This would have been due to a meteorological phenomenon since these two overprediction days did not occur for Run 2 nor Run 3. For Run 2, MDA8 ozone generally increased compared to Run 1 at all locations, which improved performance for Bayland and Clinton at the upper end of the distribution but introduced a positive bias for the other 2 sites and at the lower end of the distribution for all 4 sites. Run 3 concentrations were shifted down by approximately 2 to 8 ppb than Run 2, and the upper end of the distribution was generally underpredicted while the lower end of distribution was slightly over predicted for all 4 sites.

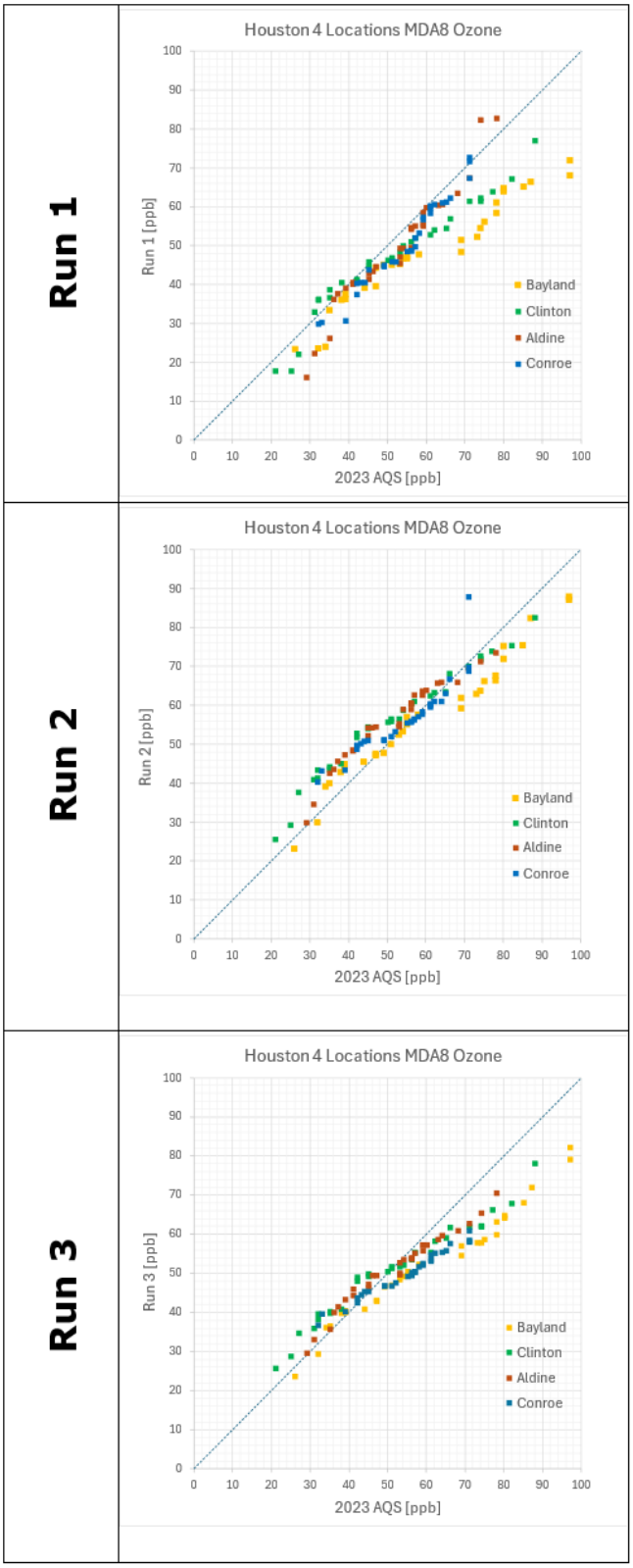

Figure 2-4. CAMx ozone model performance intra-Houston NAA Q-Q plot comparison. Run 1 (upper panel) and Run 2 (middle panel) and Run 3 (lower panel).

2.4 Dallas

2.4.1 Total Ozone

Figure 2-5 presents a comparison of September MDA8 ozone for the three CAMx model runs against 2023 observed MDA8 ozone at the primary Dallas monitor (Pilot Point). The Run 1 timeseries plot (upper left) shows different periods of relatively higher and lower MDA8 ozone, a consequence of comparing different meteorological years. The Run 1 Q-Q plot (upper right) shows consistent underpredicted ozone of approximately 5 to 15 ppb across the full range of MDA8. The Run 2 timeseries plot (middle left) shows improved temporal agreement, resulting in better ozone alignment as shown in the timeseries and also some improvement in the Q-Q plot (middle right). Table 2-4 summarizes model performance statistics and shows that Run 2 MDA8 ozone better agreed with AQS observed MDA8 ozone than Run 1 both in terms of the September mean and 4th highest MDA8. In addition, the NMB, NME and R statistics were much improved for Run 2 compared to Run 1, since the negative bias was reduced substantially, the error was smaller, and the correlation (R) was much closer to one. The improvement of Run 2 performance compared to Run 1 performance was expected since Run 2 uses 2023 meteorology, which is consistent with the 2023 AQS data. Figure 2-5 and Table 2-4 show some improvement which suggests that meteorology played a role in the Run 1 underpredictions. Differences in meteorology between 2019 and 2023 are explored in Section 3.0.

The Run 3 timeseries is generally like the Run 2 timeseries with very slightly lower values across the board. The lower Run 3 MDA8 ozone was apparent in the Q-Q plot that shows slightly more underprediction than Run 2 across the full range (i.e., for all MDA8). The Table 2-3 statistics reflect this same phenomenon and report slightly degraded model performance for Run 3 compared to Run 2 for NMB and NME but an improvement in R. This result was not expected since the updated emissions in Run 3 were developed to provide a more accurate representation of emissions which theoretically should yield improved model performance for all performance statistics. The following section explores differences in emission source group contributions to MDA8 ozone to better understand the impact of the different emissions in Run 2 versus Run 3.

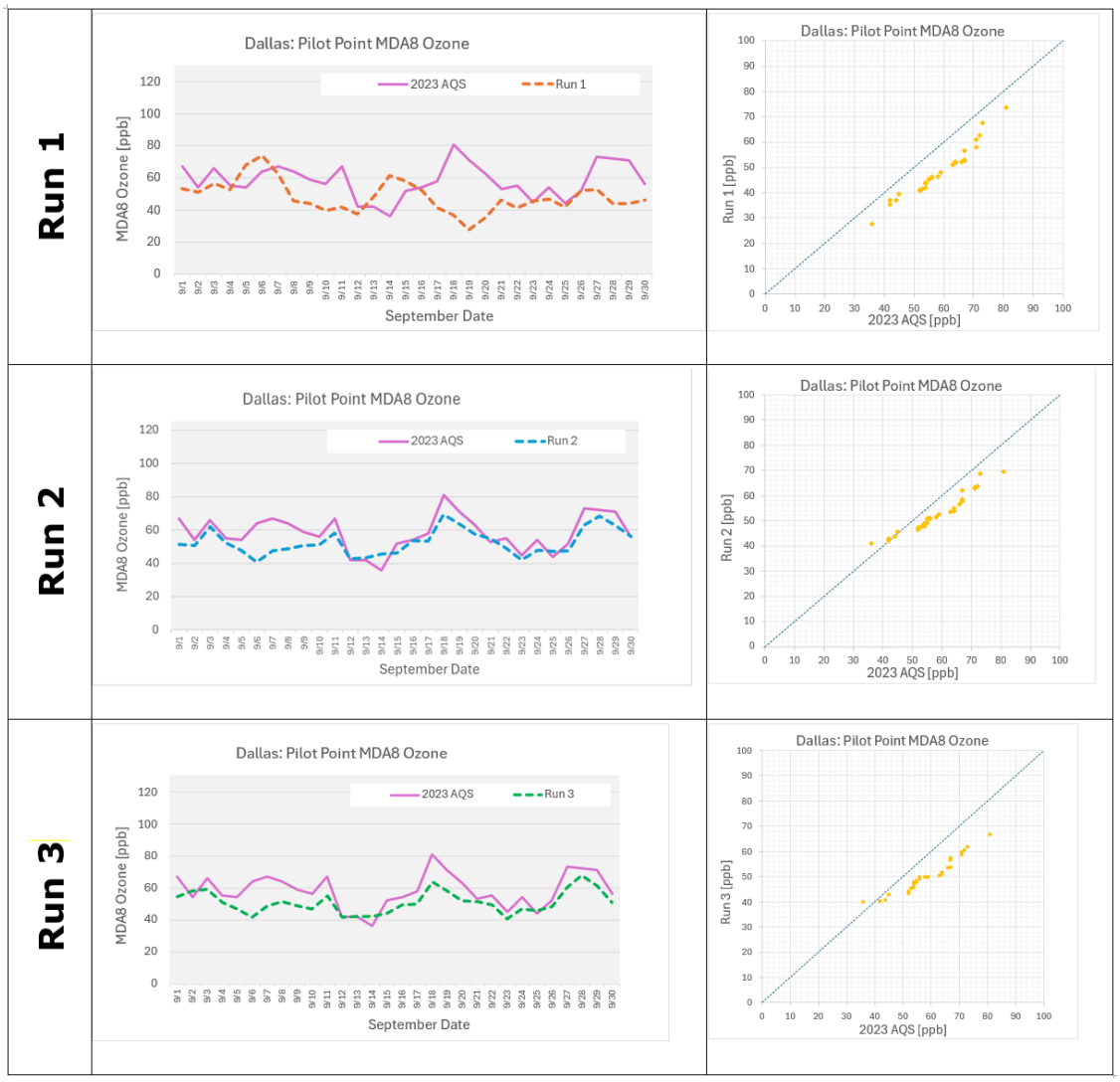

Figure 2-5. CAMx ozone timeseries and Q-Q model performance comparisons at the primary Dallas monitor (Pilot Point).

Table 2-4. CAMx model performance summary statistics for the primary Dallas area monitor (Pilot Point).

Metric	2023 AQS	Run 1	Run 2	Run 3
September Mean MDA8 [ppb]	58.2	48.2	52.6	50.9
September 4th high MDA8 [ppb]	71.0	61.2	63.1	60.3
NMB MDA8 %	-	-17.2	-9.7	-12.6
NME MDA8 %	-	24.2	11.7	14.0
R	-	-0.15	0.77	0.81

2.4.2 OSAT Emission Source Group Contributions

This section presents contributions to MDA8 ozone from different emission source groups at the Pilot Park, Dallas monitor. The same analyses for the additional Dallas monitors are provided in Appendix A.

Figure 2-6 shows Q-Q plots for CAMx OSAT source contributions to MDA8 ozone for Run 1 versus Run 2 (upper plot) and Run 2 versus Run 3 (lower plot). The "All Anthropogenic" source had the largest contribution for both meteorological years and both emissions scenarios and was approximately 10 ppb higher for Run 2 (i.e., with 2023 meteorology) than for Run 1 (i.e., with 2019 meteorology). This suggests that atmospheric transport pathways were more favorable for transport of emissions from that source category to the monitor and/or meteorological conditions were more favorable for ozone formation in 2023 compared to 2019. There are small differences in the "All Anthropogenic" contribution between Runs 2 and 3 compared to large differences between Runs 1 and 2. The biogenic contribution was greater in Run 2 as compared to Run 1 but comparable for Run 2 versus Run 3. West and east boundary contributions were generally lower for Run 2 than Run 1 while northern boundary contributions were higher and there were two days with northern boundary contributions close to or above 20 ppb for Run 2, which is quite striking since the northern boundary is thousands of kilometers from Dallas. For Run 3, there was one day with a northern boundary contribution of approximately 35 ppb. Differences in southern boundary contributions for Run 1, Run 2 and Run 3 were minimal and differences in other boundary contributions (besides one instance of north boundary contribution) between Run 2 and Run 3 were minimal. The only substantial difference between Run 2 and Run 3 was for fires, which had a much smaller contribution in Run 3 than Run 2.

Figure 2-7 provides a deeper exploration of the impact of the changes in emissions in Run 3 compared to Run 2. The boundary condition contributions were omitted, and Texas EGU and non-Texas EGU contributions are shown individually. Note that EGU emissions were adjusted in Run 3, and therefore it is important to evaluate the impact of those updated emissions. The upper and lower panels display the same data, but the lower panel "zooms in" on the smaller contributions to better discern the relatively smaller changes of the EGU contributions. The most striking observation is that Run 3 fire contributions were approximately one third of the contribution of Run 2 fire contributions, which equates to a reduction of approximately 2 - 4 ppb. This likely accounts for the lower total MDA8 ozone for Run 3 compared to Run 2, given that the other source contributions are generally comparable. A spatial map of average fire impacts is provided in a subsequent section to provide a more complete understanding of the differences in fire contributions. Texas EGU and non-Texas EGU contributions range from 0 ppb to approximately 3 ppb. The non-Texas EGU impacts were generally slightly lower for Run 3 than Run 2 (by less than 0.5 ppb) and Texas EGU impacts were mixed with variations of less than 1 ppb with more occurrences of lower contributions in Run 3 than Run 2.

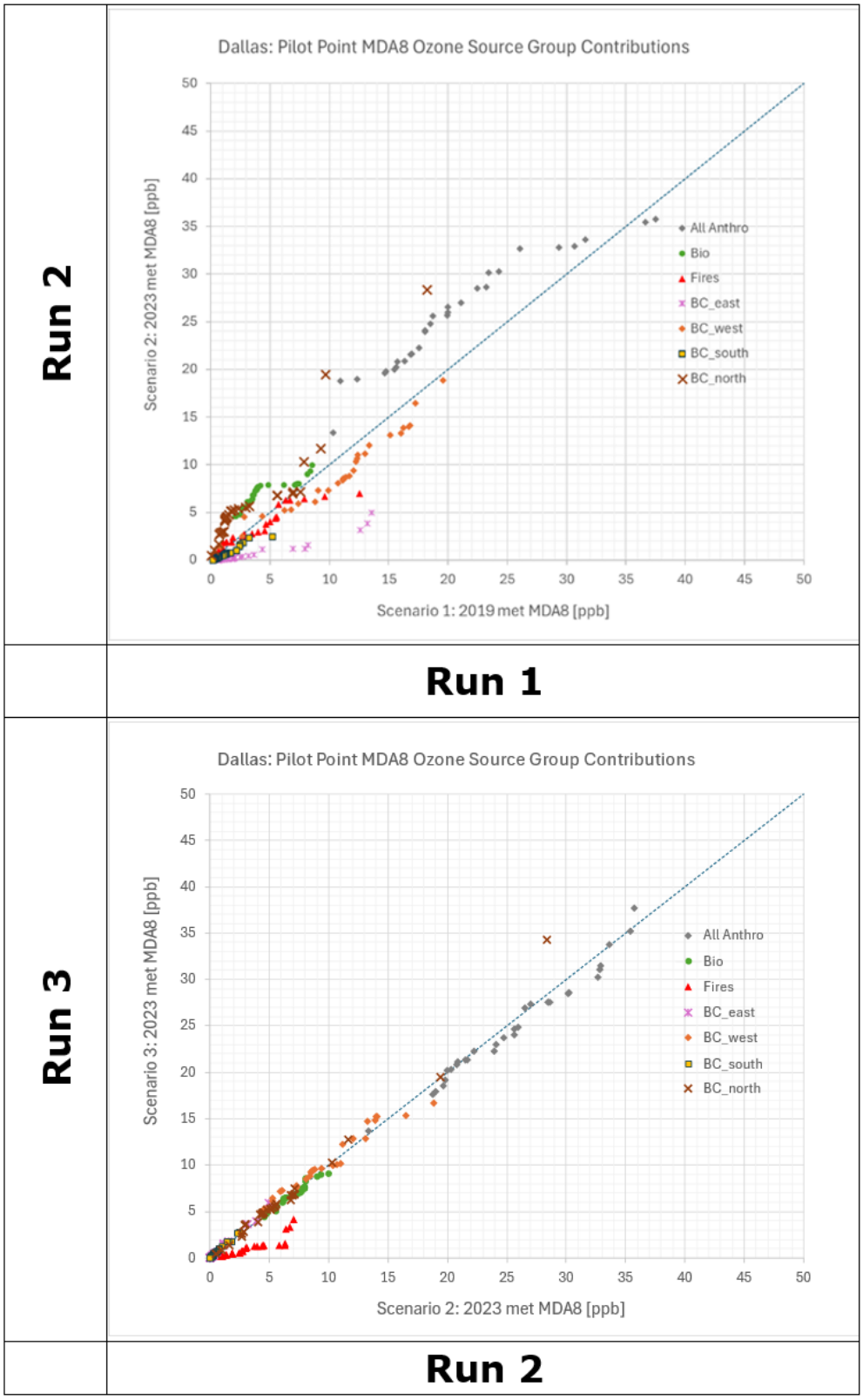

Figure 2-6. CAMx OSAT comparisons at Pilot Point, Dallas NAA. Run 1 versus Run 2 (top) and Run 2 versus Run 3 (bottom).

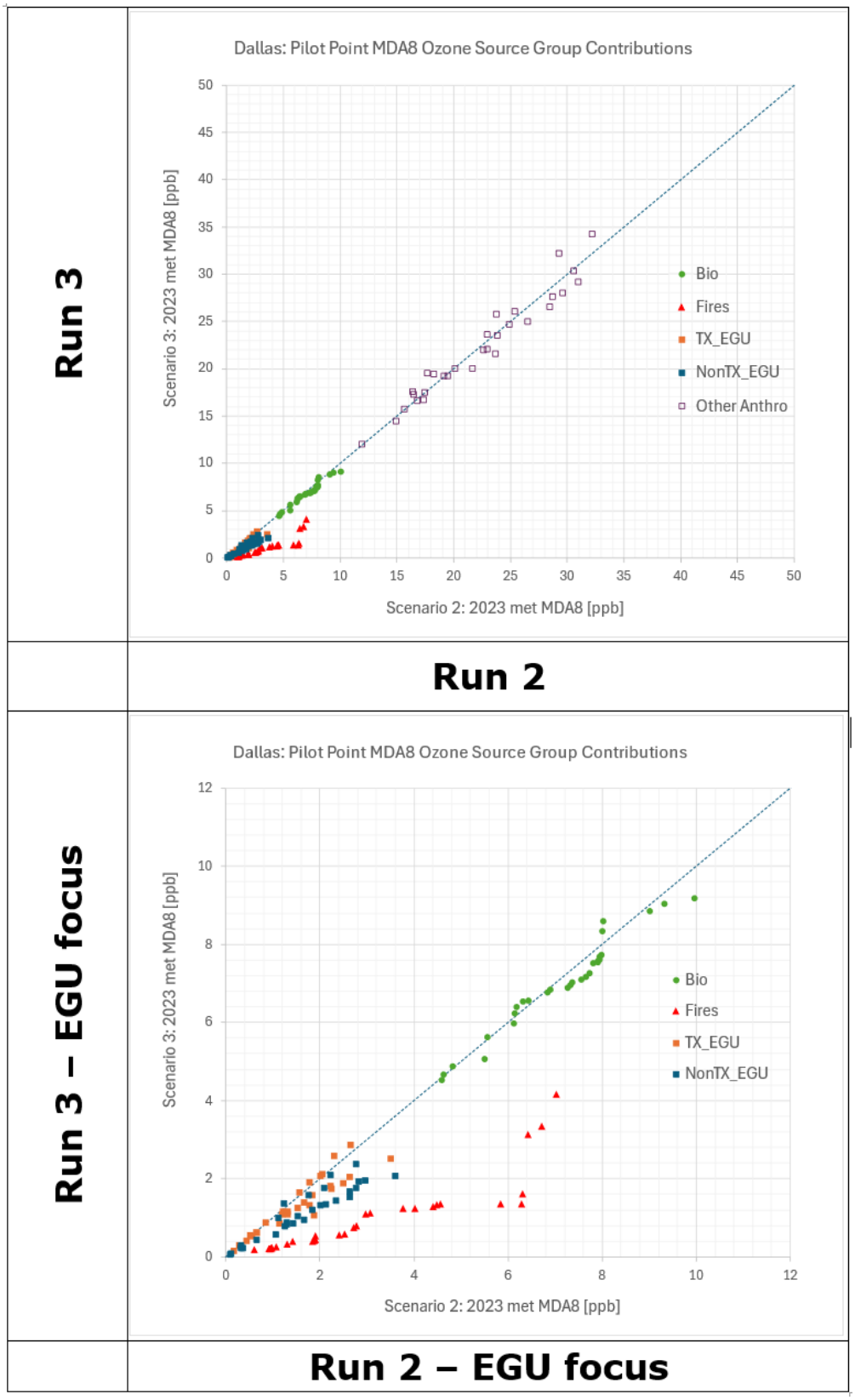

Figure 2-7. CAMx OSAT comparisons at Pilot Point, DFW NAA. Run 2 versus Run 3 with EGUs contributions separated.

2.4.3 Intra-Dallas

Appendix A reports the same analysis as shown above for the primary Pilot Park, DFW NAA monitor, but instead shows the 2 additional DFW NAA monitors. Figure 2-8 compares total MDA8 ozone results for the 3 DFW NAA monitors. Run 1 negative bias occurs at all 3 monitors and was somewhat alleviated at all 3 monitors in Run 2. The main difference between Run 2 and Run 3 was the increased negative bias in Run 3 for MDA8 greater than 50 ppb. For Run 2 and Run 3, MDA8 ozone at Fort Worth Northwest was consistently higher than for Pilot Park and Kaufman for the full range of the distribution in contrast to Run 1 which had more variability in which monitor had higher MDA8 ozone. Run 1 tended to have more negative bias for the mid-range MDA8 (i.e., 50 to 60 ppb) whereas Run 3 tended to have more negative bias at the upper MDA8 range (i.e. greater than 60 ppb). As seen in the previous analysis, the results are sensitive to meteorology and fire emissions, and these are both explored in more detail in subsequent analyses.

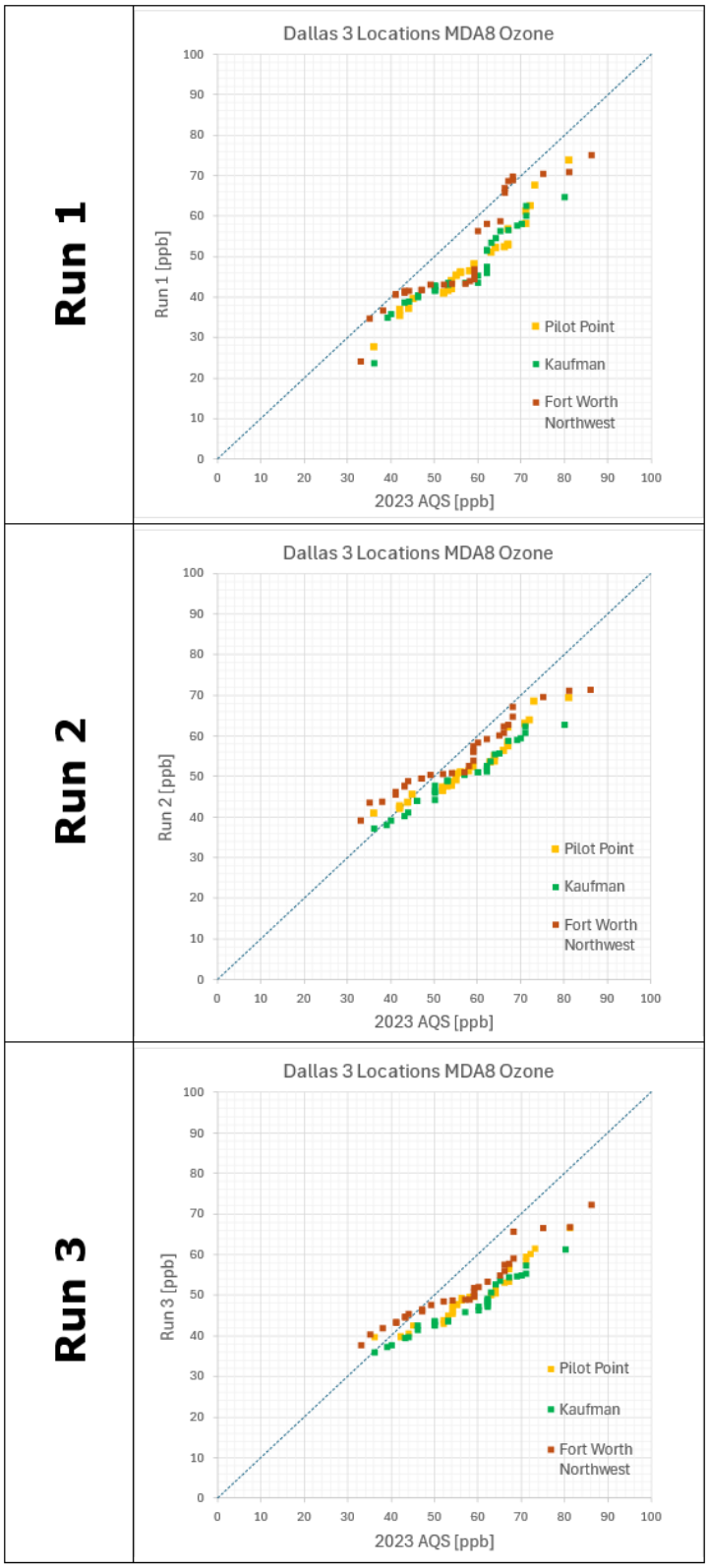

Figure 2-8. CAMx ozone model performance intra-Dallas NAA Q-Q plot comparison. Run 1 (upper panel) and Run 2 (middle panel) and Run 3 (lower panel).

2.5 San Antonio

2.5.1 Total Ozone

Figure 2-9 presents a comparison of September MDA8 ozone for the three CAMx model runs against 2023 observed MDA8 ozone at the primary San Antonio monitor (Camp Bullis). The Run 1 timeseries plot (upper left) shows different periods of relatively higher and lower MDA8 ozone, a consequence of comparing different meteorological years. The Run 1 Q-Q plot (upper right) shows substantial underpredicted ozone especially at the upper end of the range (i.e., above 60 ppb). The Run 2 timeseries plot (middle left) shows much improved temporal agreement, resulting in better ozone alignment as shown in the timeseries and a substantial improvement in the Q-Q plot (middle right). Table 2-5 summarizes model performance statistics and shows that Run 2 MDA8 ozone agrees with AQS observed MDA8 ozone better than Run 1 both in terms of the September mean and 4th highest MDA8. In addition, the NMB, NME and R statistics were much improved for Run 2 compared to Run 1, since the negative bias was reduced substantially, the error was smaller, and the correlation (R) was much closer to one. The improvement of Run 2 performance compared to Run 1 performance was expected since Run 2 uses 2023 meteorology which is consistent with the 2023 AQS data. Figure 2-9 and Table 2-5 show improved statistics, which suggests that meteorology played a substantial role in the Run 1 underpredictions. Differences in meteorology between 2019 and 2023 are explored in Section 3.0.

The Run 3 timeseries was generally similar to the Run 2 timeseries with slightly lower peak values. The lower peak values were apparent in the Q-Q plot, which shows more underprediction than Run 2 at the higher end of the range (i.e., above 60 ppb), but which is not as severe as for Run 1. The Table 2-5 statistics reflect this same phenomenon and report degraded model performance for Run 3 compared to Run 2 for NMB. This result was not expected since the updated emissions in Run 3 were developed to provide a more accurate representation of emissions, which theoretically should yield improved model performance. The following section explores differences in emission source group contributions to MDA8 ozone to better understand the impact of the different emissions in Run 2 versus Run 3.

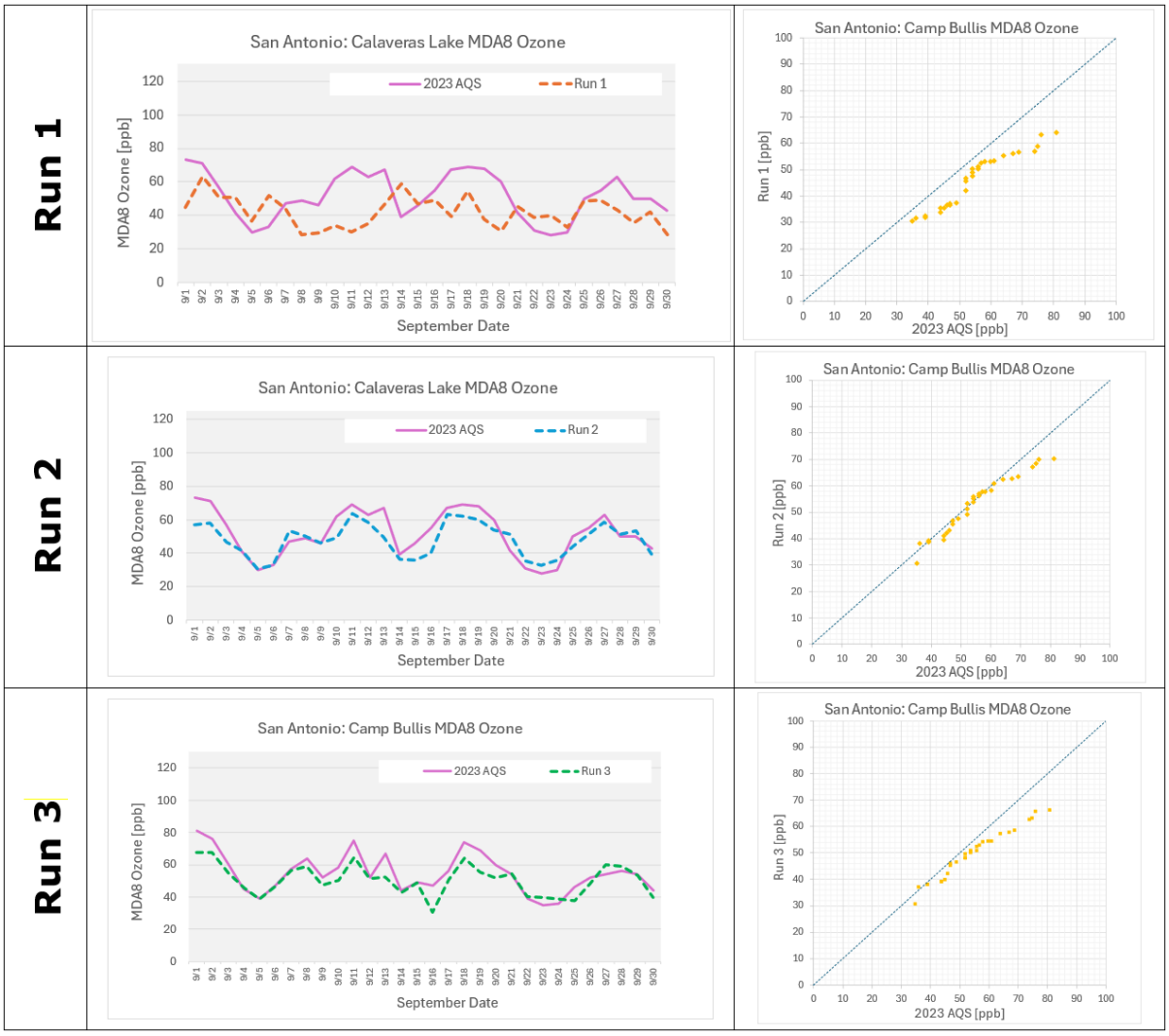

Figure 2-9. CAMx ozone timeseries and Q-Q model performance comparisons at the primary San Antonio monitor (Camp Bullis).

Table 2-5. CAMx model performance summary statistics for the primary San Antonio area monitor (Camp Bullis).

Metric	2023 AQS	Run 1	Run 2	Run 3
September Mean MDA8 [ppb]	54.8	46.2	52.8	50.6
September 4th high MDA8 [ppb]	74.0	57.0	67.2	64.0
NMB MDA8 %	-	-15.7	-3.5	-7.6
NME MDA8 %	-	25.3	8.8	9.9
R	-	0.10	0.87	0.88

2.5.2 OSAT Emission Source Group Contributions

This section presents contributions to MDA8 ozone from different emissions source groups at the Camp Bullis, San Antonio monitor. The same analyses for the additional San Antonio monitor are provided in Appendix A.

Figure 2-10 shows Q-Q plots for CAMx OSAT source contributions to MDA8 ozone for Run 1 versus Run 2 (upper plot) and Run 2 versus Run 3 (lower plot). The "All Anthropogenic" source has the largest contribution for both meteorological years and both emissions scenarios and is approximately 5 - 10 ppb higher for Run 2 (i.e., with 2023 meteorology) than for Run 1 (i.e., with 2019 meteorology). This suggests that atmospheric transport pathways were more favorable for transport of emissions from that source category to the monitor and/or meteorological conditions were more favorable for ozone formation in 2023 compared to 2019. The difference in the "All Anthropogenic" source between Run 2 and Run 3 was relatively minimal compared to Run 1 versus Run 2. The biogenic contribution was slightly larger in Run 2 as compared to Run 1 but comparable for Run 2 versus Run 3. Boundary condition contributions for the eastern, western and southern boundaries were generally lower for Run 2 than Run 1, while for the northern boundary condition they were sometimes higher for Run 2 than Run 1. Fires contributions were comparable for Run 2 and Run 1. Differences in boundary condition impacts for Run 2 and Run 3 were minimal. The only substantial difference between Run 2 and Run 3 was for fires which had a much smaller contribution in Run 3 than Run 2.

Figure 2-11 provides a deeper exploration of the impact of the changes in emissions in Run 3 compared to Run 2. The boundary condition contributions were omitted, and Texas EGU and non-Texas EGU contributions are shown individually. Note that EGU emissions were adjusted in Run 3, and therefore it is important to evaluate the impact of those updated emissions. The upper and lower panels display the same data, but the lower panel "zooms in" on the smaller contributions to better discern the relatively smaller changes of the EGU contributions. The most striking observation is the difference in fire impacts that were much smaller for Run 3 than Run 2 (i.e., a reduction of approximately 2 - 4 ppb). This likely accounts for the lower total MDA8 ozone for Run 3 compared to Run 2, given that the other source contributions were generally comparable. A spatial map of average fire impacts is provided in a subsequent section to provide a more complete understanding of the differences in fire contributions. Texas EGU and non-Texas EGU contributions ranged from 0 ppb to approximately 5 ppb and both Texas and non-Texas EGU MDA8 ozone contributions were generally slightly lower for Run 3 than Run 2 (by less than 0.5 ppb).

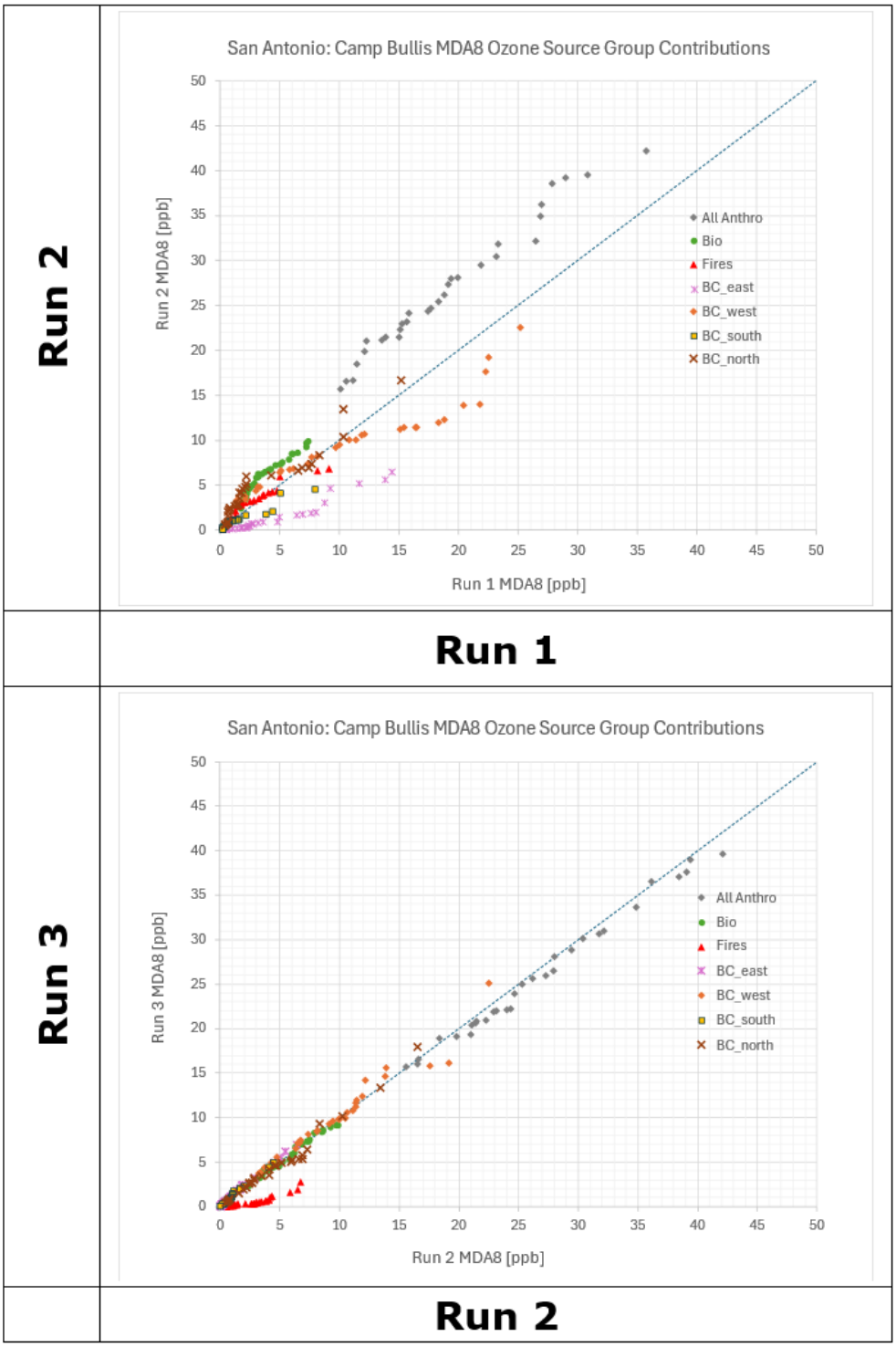

Figure 2-10. CAMx OSAT comparisons at Camp Bullis, San Antonio NAA. Run 1 versus Run 2 and Run 2 versus Run.

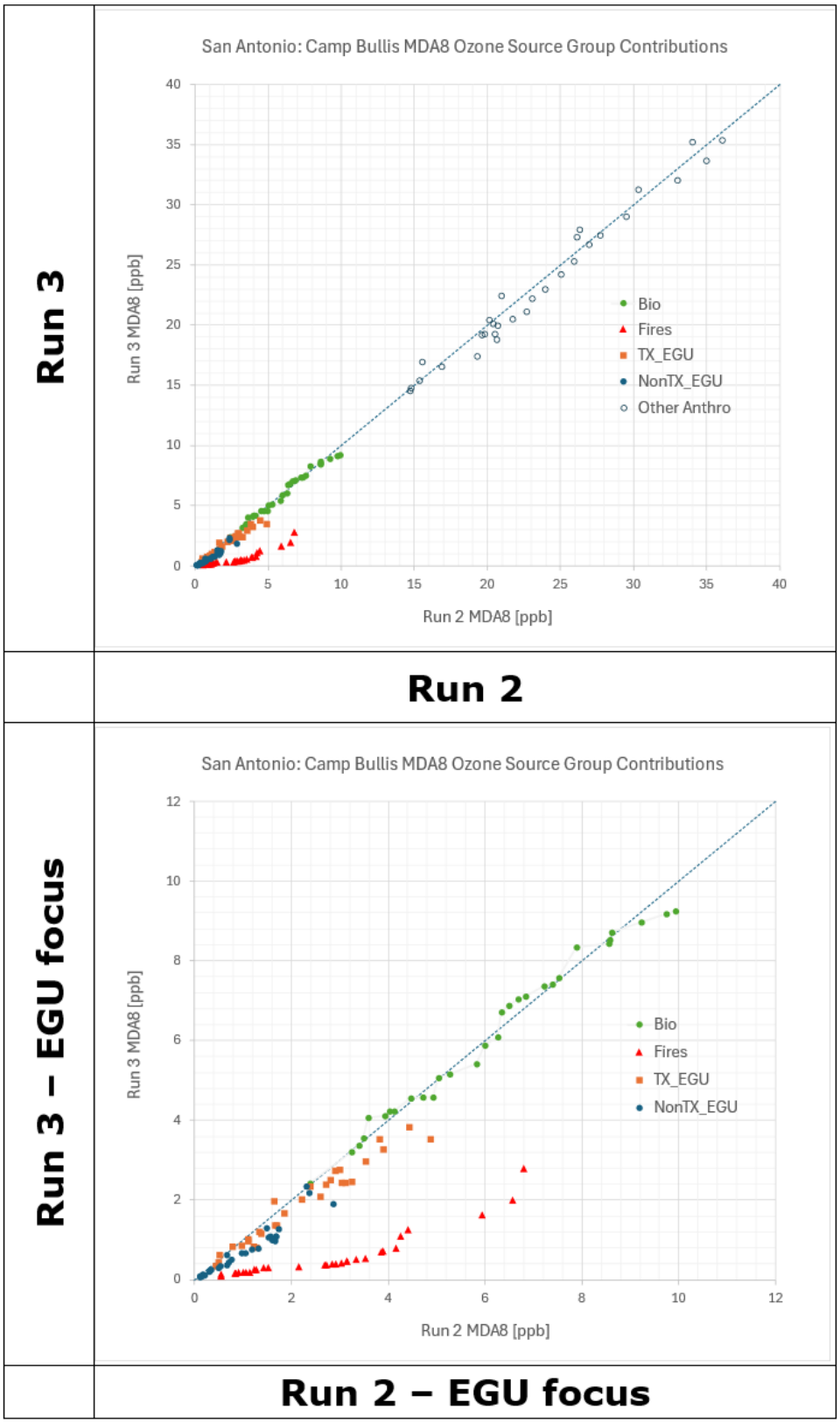

Figure 2-11. CAMx OSAT comparisons at Camp Bullis, San Antonio NAA. Run 2 versus Run 3 with EGUs contributions separated.

2.5.3 Intra-San-Antonio

Appendix A reports the same analysis as shown above for the primary Camp Bullis, San Antonio monitor but for the additional San Antonio NAA monitor. Figure 2-11 compares total MDA8 ozone results for the two San Antonio NAA monitors in terms of Q-Q plots. The Run 1 negative bias occurred at both monitors and was somewhat alleviated at both monitors for Run 2. There was little difference between Run 2 and Run 3 at both monitors except for increased negative bias in Run 3 compared to Run 2 for MDA8 greater than 50 ppb. As seen in the previous analysis, the results are sensitive to meteorology and fire emissions, and these are both explored in more detail in subsequent analyses.

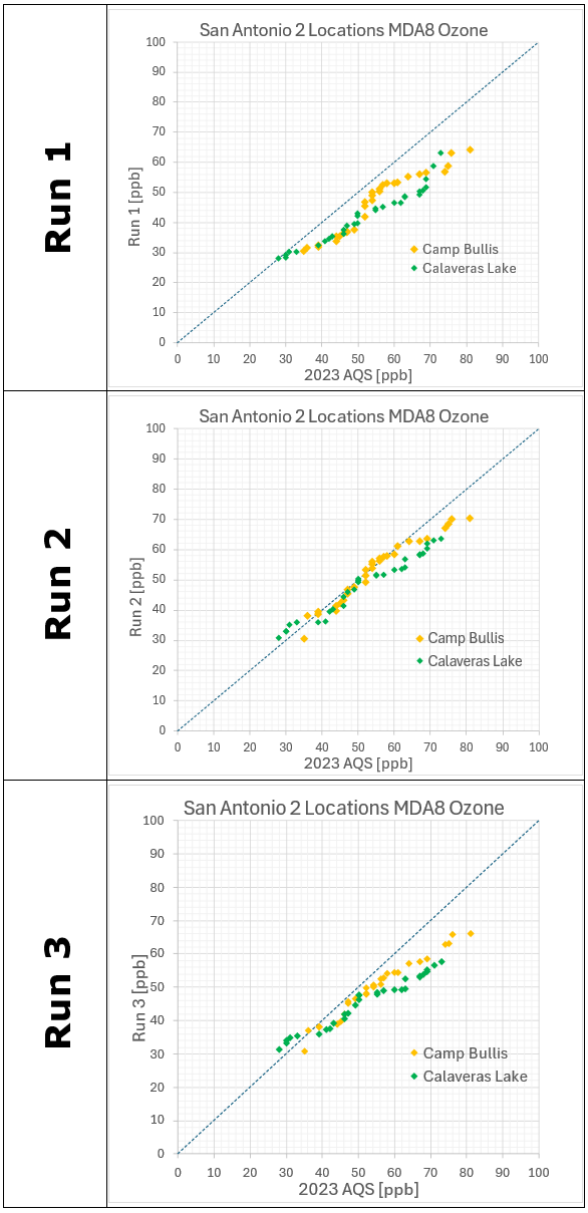

Figure 2-12. CAMx ozone model performance intra-San Antonio NAA Q-Q plot comparison. Run 1 (upper panel) and Run 2 (middle panel) and Run 3 (lower panel).

2.6 Spatial ozone maps

Figure 2-13 presents spatial maps over the 4 km CAMx modeling domain for September monthly average MDA8 ozone and September 4th highest MDA8 ozone. Increases in MDA8 for Run 2 compared to Run 1 are clearly apparent in the September average plots domain wide, including within the three outlined NAAs. Differences in 4th high MDA8 between these two runs are more variable, with Run 2 generally higher than Run 1 but by smaller margins and/or with less spatial consistency. The Run 3 monthly average MDA8 ozone spatial map generally appears more like Run 1 than Run 2 since the peak values in the NAAs are in the 50 to 55 ppb range rather than greater than 55 ppb, and most of east Texas is in the 45 – 50 ppb range rather than 50 – 55 ppb. For the 4th high MDA8 ozone all three spatial patterns are quite different. The substitution of 2019 meteorology with 2023 meteorology drove the increase in ozone concentration and meteorology played a critical role in driving the higher observed September 2023 ozone conditions in Texas. Whereas Run 3 updated multiple emission sectors, the main difference between Run 2 and 3 results can be attributed to the fire emissions.

Figure 2-14 shows a spatial map of the September average MDA8 ozone fire contribution for Run 2 and Run 3 and shows a different magnitude and spatial pattern. Run 2 had maximum fire contributions in Louisiana just across the border from East Texas and a wide region in East Texas with September average fire contributions that exceeded 3.5 ppb. However, fire contributions for Run 3 in the same region tended to be less than 1.0 ppb. Since fire emissions in Run 3 correspond to the actual modeled year they should more accurately represent day-specific fire contributions. It appears that the overestimate of fire emissions for Run 1 helped offset the negative bias and the model performance may have been even worse if the correct year fire emissions had been used. Therefore, the Run 2 model performance is better than the Run 3 model performance but for the wrong reason.

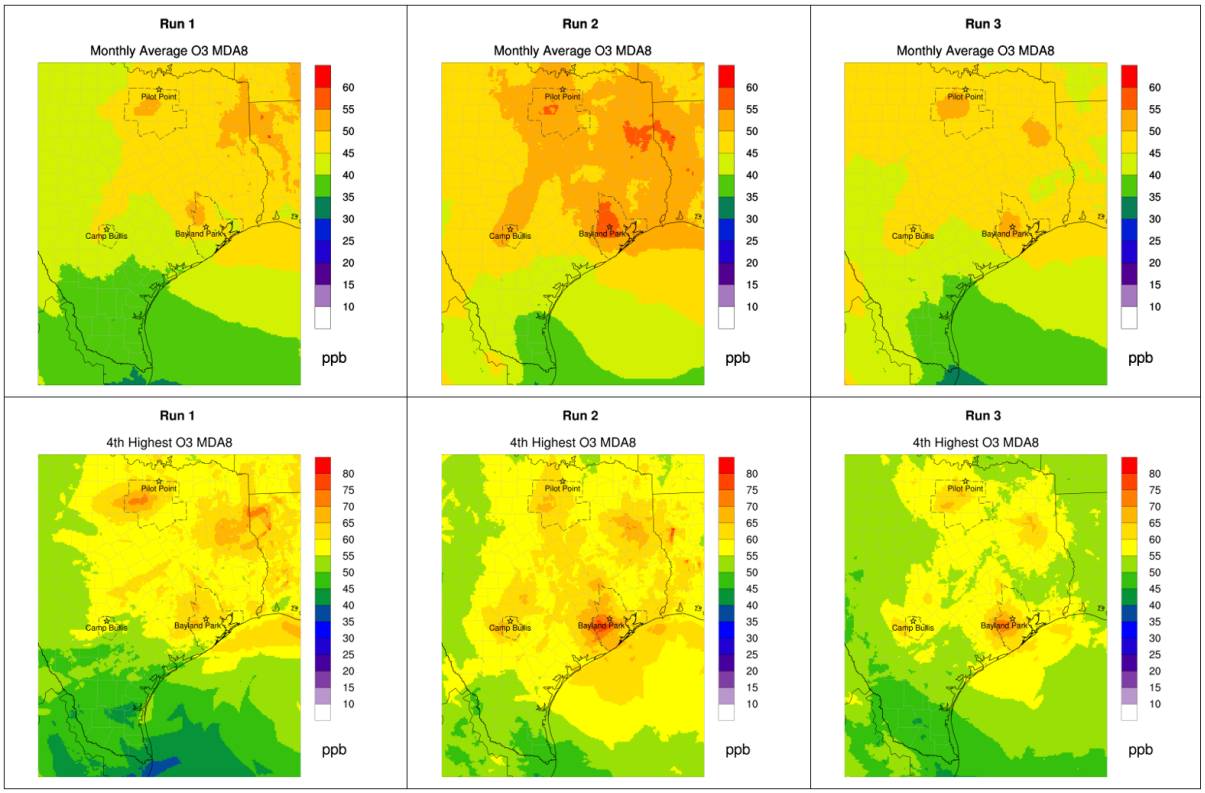

Figure 2-13. Spatial maps of CAMx MDA8 ozone for Run 1 (left), Run 2 (middle) and Run 3 (right) for September average MDA8 (upper) and September 4th highest MDA8 (lower). NAA outlines are depicted as dashed lines. Primary ozone monitor locations are shown as stars.

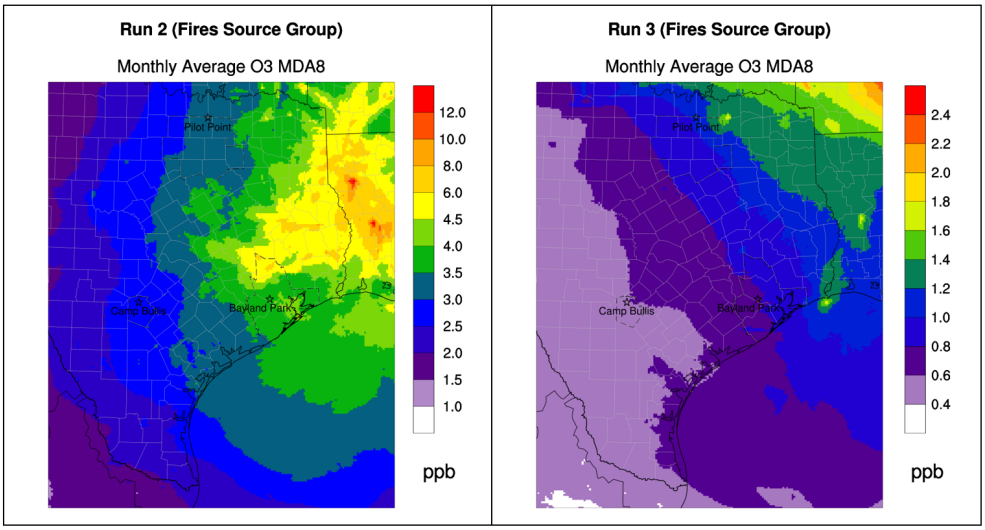

Figure 2-14. Spatial maps of CAMx OSAT fire contributions to MDA8 ozone for Run 2 (left), Run 3 (right) for September average MDA8, with different scales.

3.0 METEOROLOGICAL COMPARISON

This section examines and quantifies the difference in meteorology between 2019 and 2023 to understand the impacts to ozone transport and formation. In order to determine which meteorological parameters to focus on specifically in Texas, Ramboll reviewed conceptual model analyses from recent State Implementation Plan (SIP) revisions for HGB,[3] DFW,[4] and San Antonio.[5] The main findings from the conceptual models are presented in Figure 3-1, Figure 3-2, and Figure 3-3 for HGB, DFW, and San Antonio (Bexar County), respectively.

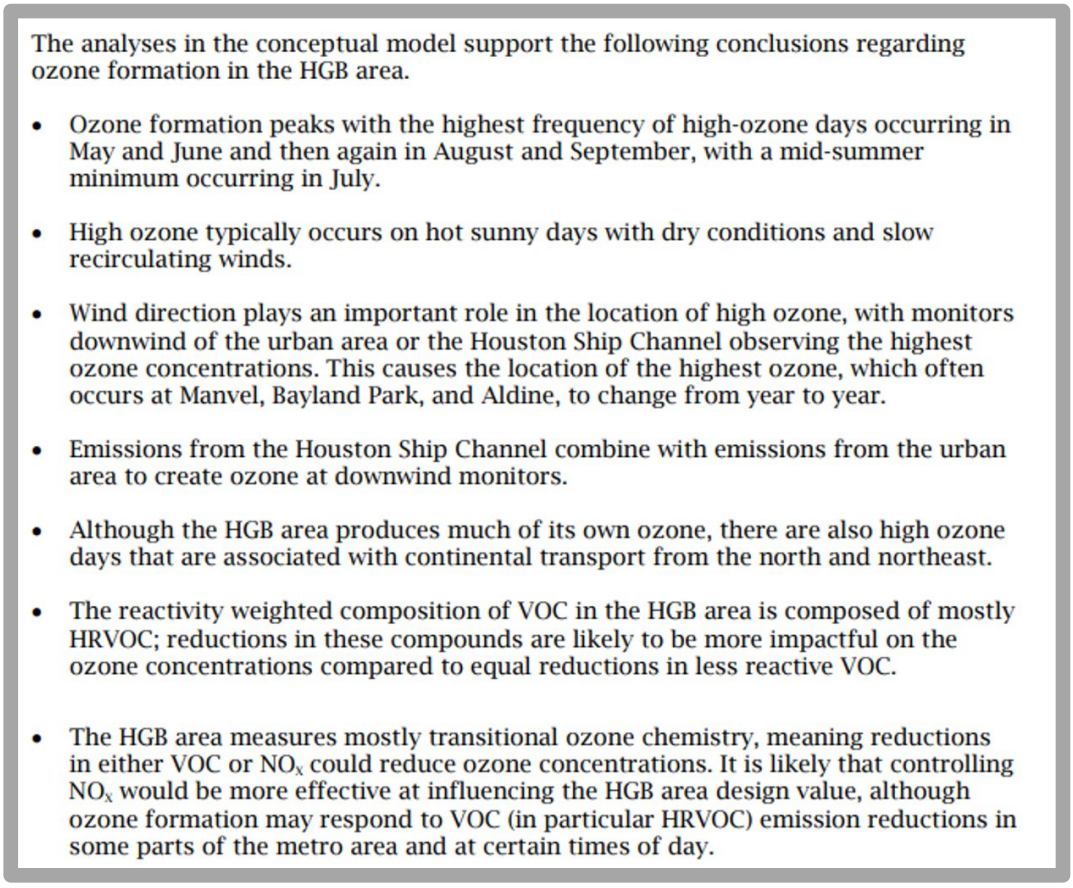

The analyses in the conceptual model support the following conclusions regarding ozone formation in the HGB area.

- Ozone formation peaks with the highest frequency of high-ozone days occurring in May and June and then again in August and September, with a mid-summer minimum occurring in July.
- High ozone typically occurs on hot sunny days with dry conditions and slow recirculating winds.
- Wind direction plays an important role in the location of high ozone, with monitors downwind of the urban area or the Houston Ship Channel observing the highest ozone concentrations. This causes the location of the highest ozone, which often occurs at Manvel, Bayland Park, and Aldine, to change from year to year.
- Emissions from the Houston Ship Channel combine with emissions from the urban area to create ozone at downwind monitors.
- Although the HGB area produces much of its own ozone, there are also high ozone days that are associated with continental transport from the north and northeast.
- The reactivity weighted composition of VOC in the HGB area is composed of mostly HRVOC; reductions in these compounds are likely to be more impactful on the ozone concentrations compared to equal reductions in less reactive VOC.
- The HGB area measures mostly transitional ozone chemistry, meaning reductions in either VOC or NO_x could reduce ozone concentrations. It is likely that controlling NO_x would be more effective at influencing the HGB area design value, although ozone formation may respond to VOC (in particular HRVOC) emission reductions in some parts of the metro area and at certain times of day.

Figure 3-1. HGB conceptual model summary excerpted from the HGB SIP.

[3] https://www.tceq.texas.gov/downloads/air-quality/sip/ozone/houston/naaqs-2008/23110sip_2008o3_hgb-sev-ad_ado_appb_conceptualmodel.pdf

[4] https://www.tceq.texas.gov/downloads/air-quality/sip/ozone/dfw/naaqs-2008/23107sip_2008dfw_sev_ad_appb_conceptualmodel_ado.pdf

[5] https://www.tceq.texas.gov/downloads/air-quality/sip/ozone/san-antonio/2015-naaqs/24041sip_2015_bex-serious-ad_app-b_conceptual-model_aqd-approved.pdf

This conceptual model supports the following conclusions regarding ozone formation in the DFW area:

- Ozone formation peaks with the highest frequency of high-ozone days occurring from April through June and then again from August through October, with a mid-summer minimum occurring in July. This minimum results from the location of the Bermuda High, a high-pressure system that brings clean air from the Gulf of Mexico into the DFW area in the mid-summer.
- High ozone typically occurs on hot sunny days with dry conditions and slow winds out of the southeast.
- Emissions located south and southeast of the DFW area combine with urban area emissions to create ozone, which is carried to monitors in the north and northwest portions of the DFW area.
- Ozone can be exacerbated by slow and variable winds that recirculate air on high ozone days.
- Meteorological conditions that create high local ozone formation potentially also create high regional background ozone, which combines with local emissions to produce eight-hour ozone levels above 75 ppb.
- Ozone chemistry in the DFW area appears to be NO_x limited to transitional. The dominant VOC in the area are either naturally occurring isoprene from vegetation, or have low ozone formation potential; therefore, control of VOC would have less effect on ozone concentrations in the DFW area compared to NO_x controls.

Figure 3-2. DFW conceptual model summary excerpted from the DFW SIP.

The analyses conducted for this conceptual model support the following conclusions regarding ozone formation in the Bexar County 2015 ozone NAAQS nonattainment area.

- Ozone concentrations peak from May through June and then again from August through October, with a mid-summer minimum occurring in July. The latter half of the ozone season generally sees higher ozone than the first half.
- High ozone typically occurs on hot, sunny days with dry conditions and slow wind speeds out of the southeast or northeast. The highest ozone days often have recirculating winds that exacerbate ozone accumulation.
- The synoptic-scale meteorological conditions that allow for high local ozone formation also create high levels of regional background ozone, which combines with the locally formed ozone and emissions to produce eight-hour ozone levels greater than 70 ppb.
- Emissions located south, southeast, and east of the Bexar County 2015 ozone NAAQS nonattainment area combine with urban-area mobile source emissions to create ozone which are then transported to the monitors located in the northwest portion of the Bexar County 2015 ozone NAAQS nonattainment area.
- Ozone formation appears to be predominantly NO_x limited at the monitors with the highest ozone concentrations in the Bexar County 2015 ozone NAAQS nonattainment area.

Figure 3-3. San Antonio conceptual model summary excerpted from the Bexar County SIP (San Antonio).

According to all three conceptual models, high ozone typically occurs on hot, sunny days with dry conditions and slow winds. Therefore, in the following analysis, Ramboll evaluated parameters related to these characteristics. Ramboll also evaluated planetary boundary layer (PBL) height since this is known to influence air pollution concentrations due to the degree of vertical mixing that occurs within deep versus shallow boundary layers. The meteorological parameters were examined using two complementary approaches:

1. Regional monthly climatology and anomalies:

Ramboll obtained climatology and anomaly data from the National Oceanic and Atmospheric Administration (NOAA) National Centers for Environmental Prediction (NCEP) Physical Sciences Laboratory (PSL) Reanalysis 1 dataset,[6,7] specifically the monthly/seasonal climate composite analyses.[8] Note the climatology used for the anomaly and long term mean plots were recently updated to 1991-2020 to match the new climate "normal" time period. All climate and anomaly analyses are for September only. The NCEP/NCAR Reanalysis 1 project uses a state-of-the-art analysis/forecast system to perform data assimilation using past data from 1948 to the present. The resulting analyses were prepared for the contiguous U.S. The climatology provides context for each meteorological parameter and the anomalies show the deviations from typical conditions for each meteorological parameter for each year of 2019 and 2023. Since these analyses are based on September averages, intramonthly variations are obscured, however, important features and differences between the years are evident.

2. Hourly and/or daily analysis at primary and supplementary NAA monitor locations

We extracted hourly meteorological parameters from the input data used to drive CAMx for Run 1, Run 2 and Run 3, which are based on TCEQ's application of the Weather Research and Forecasting (WRF) model.[9] Meteorological parameters were extracted at the three grid cell locations that correspond to the primary ozone monitors and the six grid cell locations that correspond to the supplementary ozone monitor locations. For some parameters, Ramboll evaluated hourly statistics and for others, daily mean or maximum statistics were evaluated as they are more relevant to ozone formation, as explained in each section below. The following meteorological parameters were evaluated:

- Temperature
- Solar radiation and/or model cloudiness
- Relative humidity (climatology only)
- Wind speed and direction (surface level, aloft for climatology)

[6] *NCEP-NCAR Reanalysis 1 data provided by the NOAA PSL, Boulder, Colorado, USA, from their website at https://psl.noaa.gov*

[7] NCEP/NCAR Reanalysis at PSL: NOAA Physical Sciences Laboratory

[8] Monthly/Seasonal Composites: NOAA Physical Sciences Laboratory

[9] https://nuwrf.gsfc.n asa.gov/wrf

- Planetary boundary layer height

3.1 Temperature

The regional climate/anomaly analysis shows that throughout Texas both 2019 and 2023 exhibited positive temperature anomalies (approximately 2-4 degrees Celsius), with the highest occurring in northern Texas in 2019 and southwestern Texas in 2023 (Figure 3-4). The temperature anomalies along the Gulf Coast including Houston were relatively consistent in both years. The much more expansive 2023 anomaly across Texas would be a key contributor to higher ozone in 2023 than 2019.

Figure 3-5 presents time series of simulated and observed daily maximum temperatures (Kelvin)[10] for September 2019 and 2023 at DFW, San Antonio, and HGB primary monitors. All locations had many warmer days in September 2023 than September 2019, with the highest 2023 temperatures occurring around the 7th and 8th of September. A cooler period occurred during the 10th to the 15th of September 2023, but the last 10 days of the month were warmer again. Daily maximum temperatures were well simulated for each NAA (i.e., within 0 to 2 degrees Celsius) with a general tendency for slight overprediction in both years.

Figure 3-6 presents the statistical comparison of 2023 vs. 2019 simulated daily maximum temperatures within the three NAAs as Q-Q plots, along with the intra-NAA variation across the additional monitors. These plots show consistently higher temperatures at the upper end of the range at all locations in 2023 compared to 2019, and mixed differences between the sites for the cooler days. These distinct NAA characteristics are quite uniform within each NAA; i.e., there are clear differences between the three NAAs but minimal differences for the set of monitors within each NAA.

The higher peak temperatures and higher frequency of warm days in 2023 likely contributed to higher ozone that year. Meteorological model performance for temperature likely played a minor role in the 2023 underestimate of ozone given that magnitudes and inter-daily variability were fairly well simulated (i.e., within approximately 1-degree Celsius) yet slightly over estimated.

[10] To convert to Celsius apply the conversion: C = K - 273.15

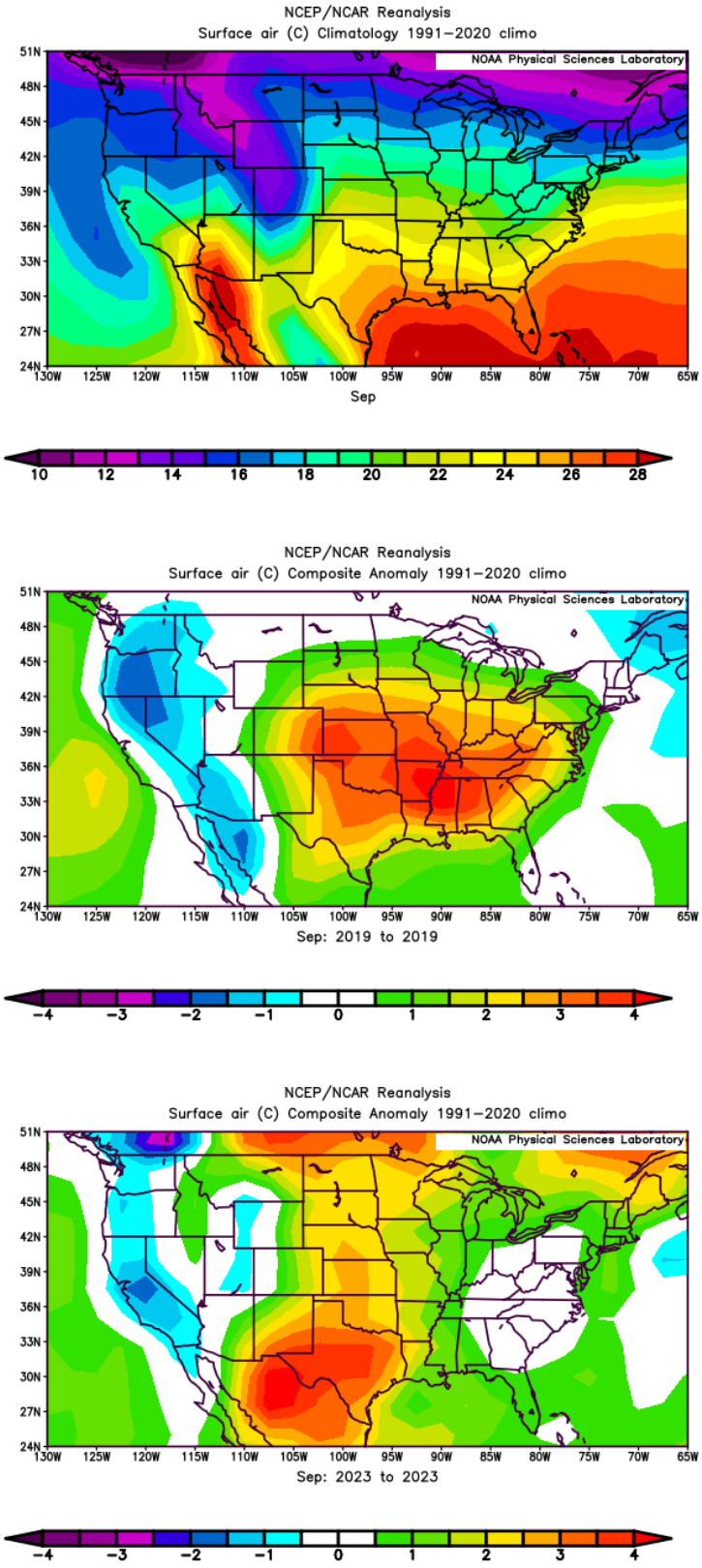

Figure 3-4. Temperature climatology based on 1981-2020 (top) and anomalies in 2019 (middle) and 2023 (bottom).

Figure 3-5. Simulated and observed daily maximum temperature at Dallas (top), San Antonio (middle), and Houston (bottom) during September 2019 and September 2023.

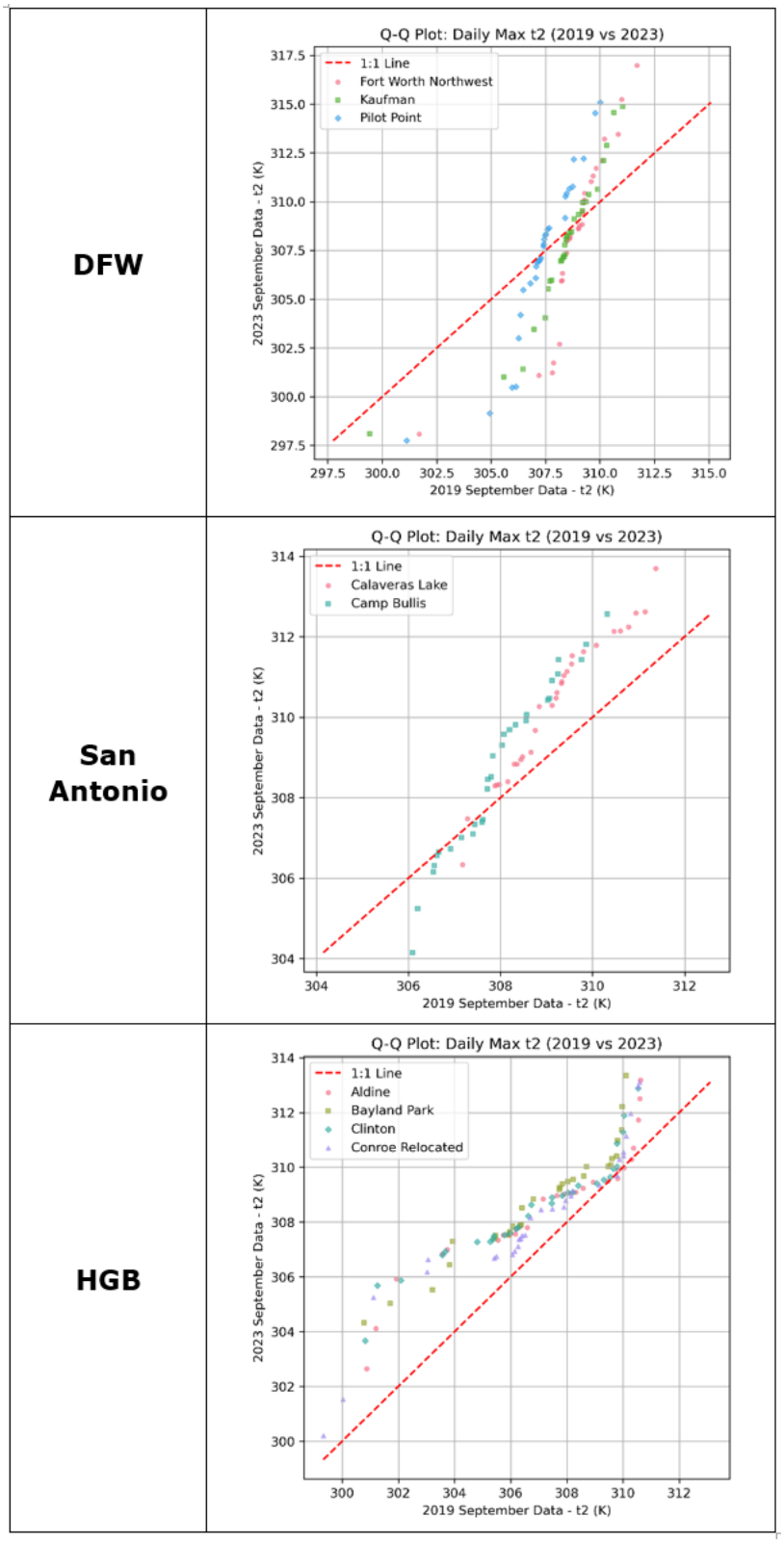

Figure 3-6. Q-Q plot showing intra-NAA comparisons of simulated daily maximum temperatures in 2023 versus 2019 for DFW (top), San Antonio (middle) and HGB (bottom).

3.2 Solar Radiation

The regional climate/anomaly analysis shows that throughout Texas both 2019 and 2023 exhibited slightly positive solar flux anomalies, with the highest occurring in northeastern Texas in 2019 and southern Texas in 2023 (Figure 3-7). The patterns are roughly similar to the temperature anomalies. Overall, 2023 had marginally more solar flux than in 2019.[11]

Figure 3-8 presents time series of simulated hourly cloud optical depth (cloud cover) over September 2019 and 2023 at DFW, San Antonio, and HGB primary monitors. Cloud optical depth is a unitless measure of how much light is blocked or scattered by clouds; it is generally inversely proportional to downward solar radiation. Observations were not added to these figures since the cloud optical depth is not a measured meteorological parameter. Simulated hourly cloud cover was generally lower and less frequent at HGB and San Antonio in 2023 than in 2019.

Figure 3-9 presents Q-Q plots comparing 2023 versus 2019 for the three NAA including supplementary sites to show intra-NAA differences. Note that high ozone occurs more frequently on sunny days, which corresponds to lower cloud cover, so the most relevant observations in these figures are for low cloud cover. San Antonio and HGB had much less cloud cover at all locations in 2023 compared to 2019. Dallas had similar cloud cover in 2019 and 2023 (in agreement with the solar radiation analysis in Figure 3-7). It is unclear why DFW has more intra-NAA deviation (i.e., Fort Worth northwest) but since this was for cloudier hours (i.e., with less solar radiation) this is not likely to impact the high ozone days.

Higher levels of solar radiation and higher frequency of cloud free conditions for HGB and San Antonio in 2023 compared to 2019 likely contributed to higher ozone photochemistry in the later year.

[11] This analysis product is not available for the more recent climate period and was obtained from the NCEP North American Regional Reanalysis (NARR).

NCEP NARR Monthly/Seasonal Composites: NOAA Physical Sciences Laboratory

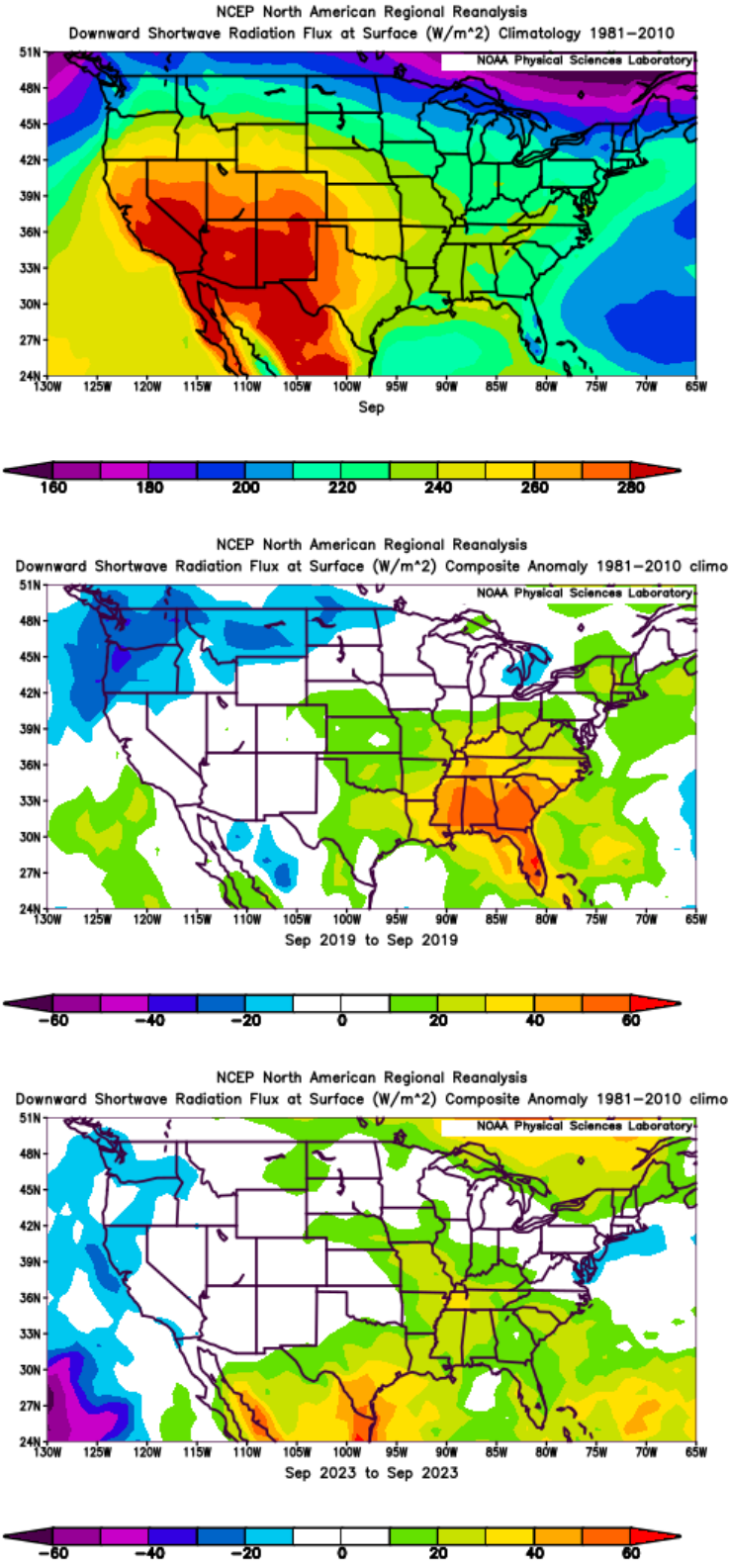

Figure 3-7. September monthly mean solar radiation climatology (top) and anomalies in 2019 (middle) and 2023 (bottom).

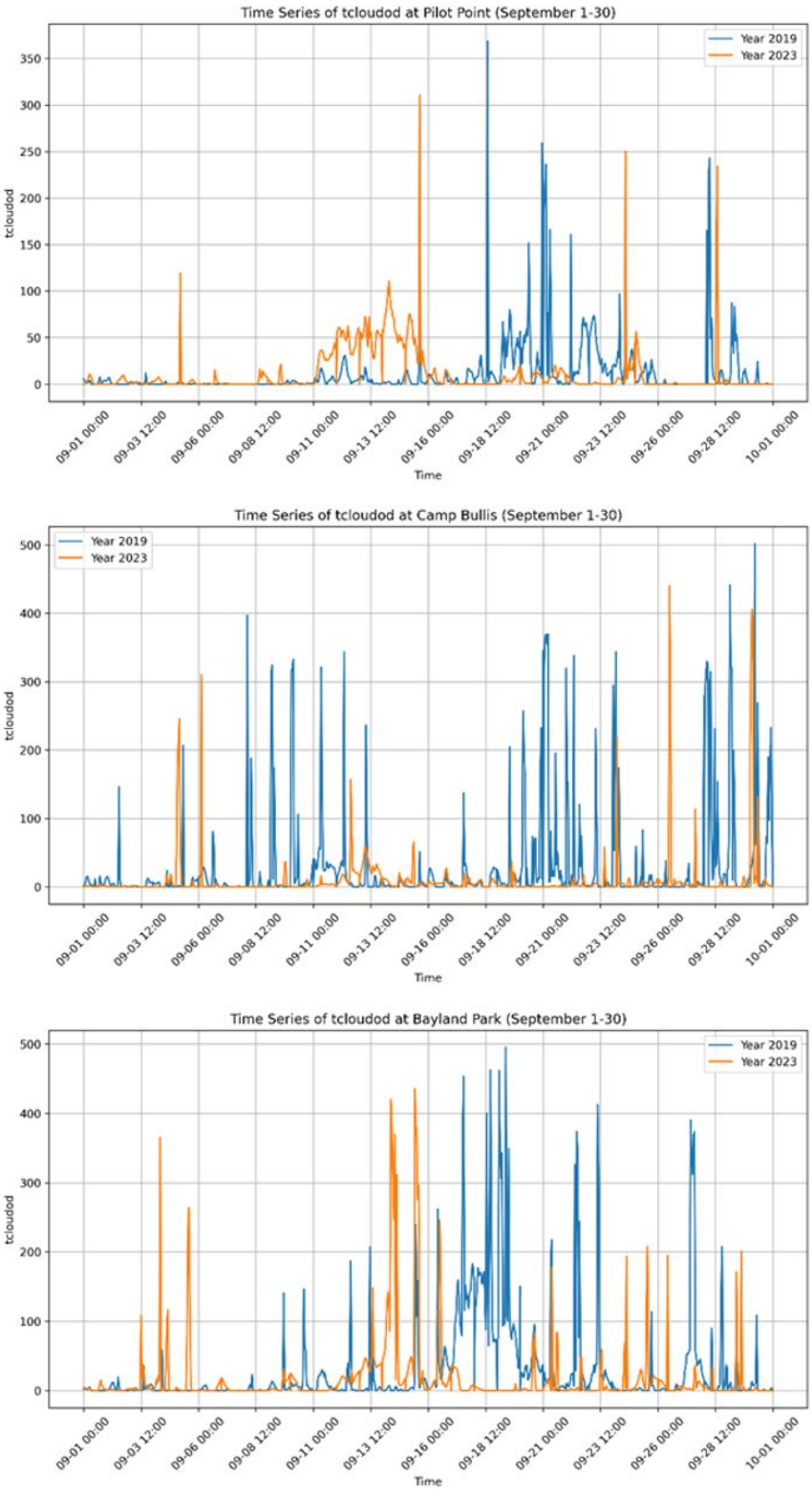

Figure 3-8. Simulated hourly cloud optical depth (unitless) at Dallas (top), San Antonio (middle), and Houston (bottom) during September 2019 and September 2023.

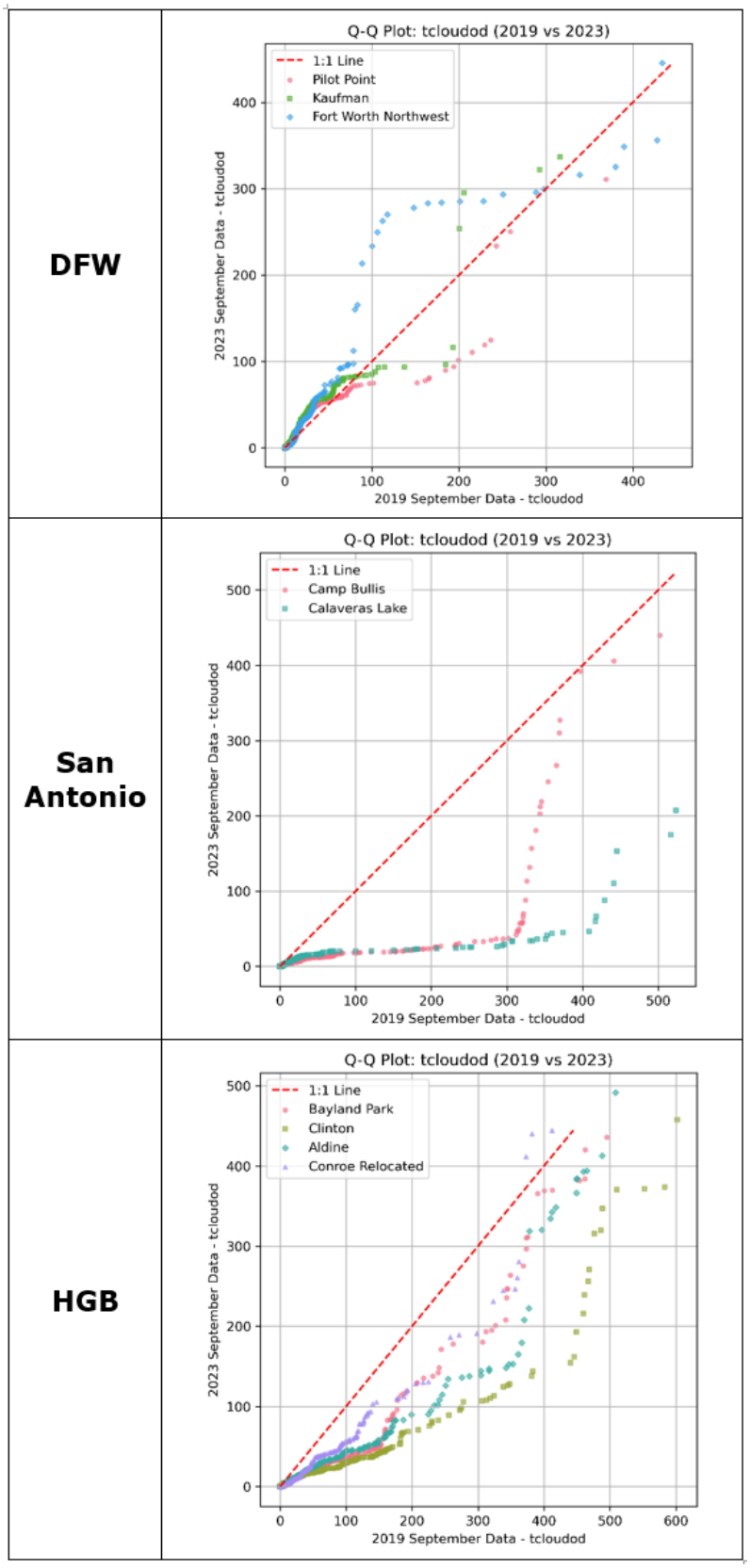

Figure 3-9. Q-Q plot showing intra-NAA comparisons of cloud optical depth in 2023 versus 2019 for DFW (top), San Antonio (middle) and HGB (bottom).

3.3 Relative humidity

The regional climate/anomaly analysis in Figure 3-10 shows that both September 2019 and September 2023 had negative relative humidity anomalies throughout Texas. This indicates that September for both years was drier than what was typical during the 1981 to 2020 period. The negative anomaly was more widespread and substantial in 2023 than in 2019. Relative humidity anomalies along the Gulf Coast including Houston were within approximately ± 2% in 2019 and about 5% to 10% lower in 2023, which was less substantial than other regions of the state. Simulated relative humidity is not presented since it is not directly modeled in WRF or CAMx. It can be calculated from modeled temperature and absolute humidity, but those calculations carry a high degree of uncertainty as they are very sensitive to errors in both parameters. Dryer conditions are associated with higher ozone levels as described in the conceptual models at the beginning of this section, and therefore, 2023 was more conducive to high ozone in terms of relative humidity.

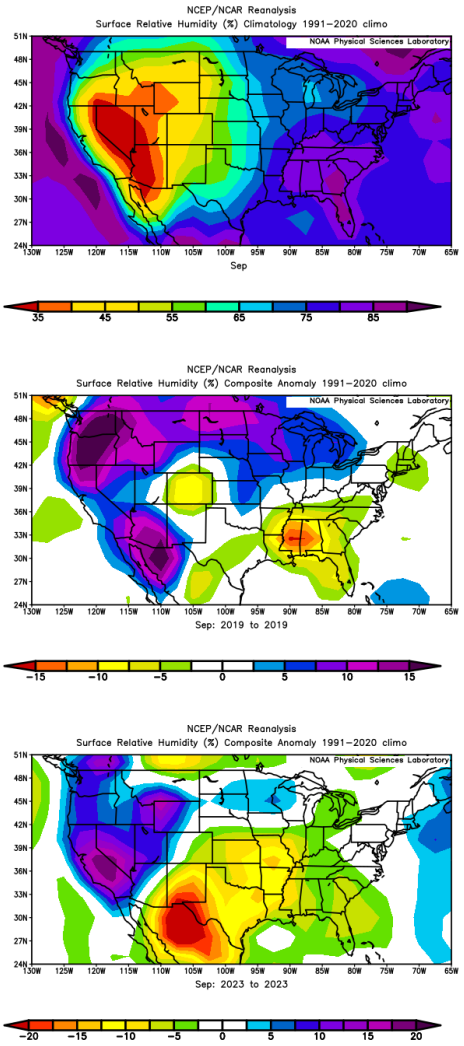

Figure 3-10. Relative humidity climatology (top) and anomalies in 2019 (middle) and 2023 (bottom).

3.4 Winds

This section evaluates differences in surface wind speeds, 850 millibar (mb)[12] meridional (south-to-north) winds, and 850 mb vector winds between September 2019 and September 2023 throughout Texas. The climatology and anomalies are presented for surface scalar wind speed and 850 mb meridional winds in Figure 3-11 and 850 mb wind vectors (over Texas only for clarity) in Figure 3-12. In September 2019, surface winds (i.e., Figure 3-11 (left panels)) were about 0.5 to 1.5 m/s faster than climatology over much of Texas, while in September 2023 they were more similar to climatology over most of Texas (i.e., within $\pm$ 0.25 m/s over much of Texas and approximately 0.5 m/s faster for northeast Texas only). Additionally, surface winds in 2023 over the Gulf of Mexico were approximately 1 to 2 m/s slower than normal. Meridional winds at 850 mb were high for most of Texas in 2019 but closer to typical in 2023. Meridional winds are related to Bermuda High, which brings cleaner Gulf of Mexico air to Texas.[13]

The 850 mb wind vector anomalies (Figure 3-12) in 2019 show increased transport from the Gulf of Mexico compared to 2023, especially over the Houston area. This is likely to be a major influence that contributed to higher ozone formation in 2023 compared to 2019.[14] Higher wind speeds, especially meridionally, in 2019 indicate more ventilation of emissions, transport of cleaner air from the Gulf of Mexico (especially in Houston), and less stagnation that can lead to the buildup of regional ozone.

Figure 3-13 presents time series of simulated and observed daily mean surface level wind speeds for September 2019 and 2023 at DFW, San Antonio, and HGB primary monitors. The most consistent feature for all years and locations is that the simulated wind speeds tended to overpredict the observed wind speeds for both slow and fast wind speed days. This could contribute to lower modeled ozone compared to observations for all runs and particularly for Runs 2 and 3 since they are the runs with matched meteorological years.

Figure 3-14 shows Q-Q plots comparing 2023 versus 2019 based on hourly winds and provides an intra-NAA analysis. All NAAs had overall slightly slower wind speeds in 2023 compared to 2019. Note that high ozone occurs more frequently on stagnant days which corresponds to slower wind speeds, so the most relevant observations in these figures are for the low wind speeds. For slower winds, the Dallas NAA had similar speeds in 2023 as 2019, while within the San Antonio and HGB NAAs there were slower winds in 2023 compared to 2019.

Two important conclusions can be gleaned from this section: (1) slower winds in 2023 compared to 2019 (especially meridional as seen in the climate/anomaly analysis) would

[12] equivalent to hectopascal (hPa)

[13] https://forecast.weather.gov/glossary.php?word=bermuda+high

[14] This analysis product is not available for the more recent climate period and was obtained from the NCEP North American Regional Reanalysis (NARR). NCEP NARR Monthly/Seasonal Composites: NOAA Physical Sciences Laboratory

suggest higher ozone in 2023; (2) comparison of simulated versus observed daily mean wind speed shows a substantial positive bias in each NAA that likely contributes to the low bias in ozone (i.e., faster winds lead to more ventilation of emissions and less stagnation and buildup of regional ozone).

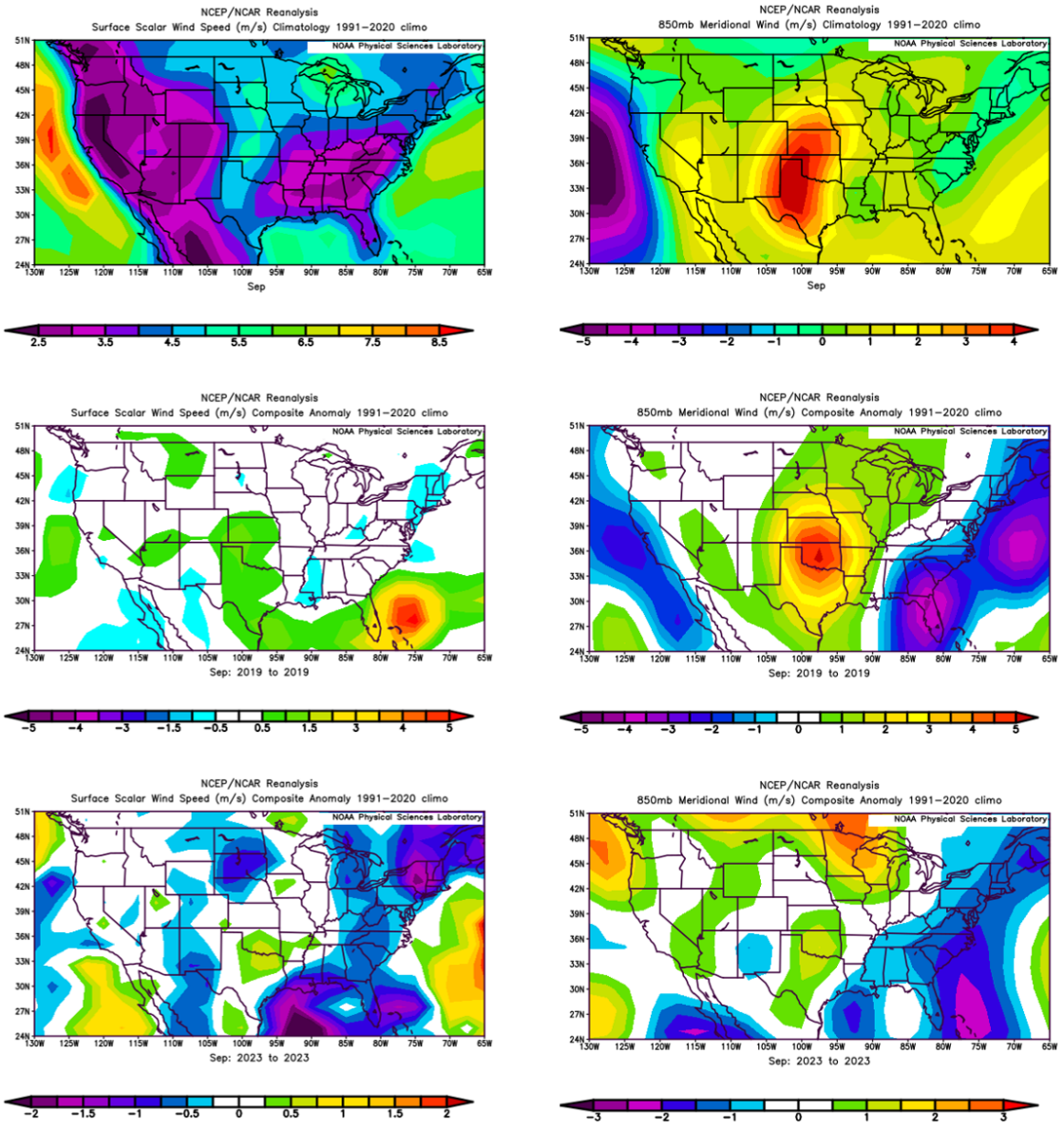

Figure 3-11. Surface wind speed climatology (top left) and anomalies in 2019 (middle left) and 2023 (bottom left). 850 mb meridional wind speed climatology (top right) and anomalies in 2019 (middle right) and 2023 (bottom right).

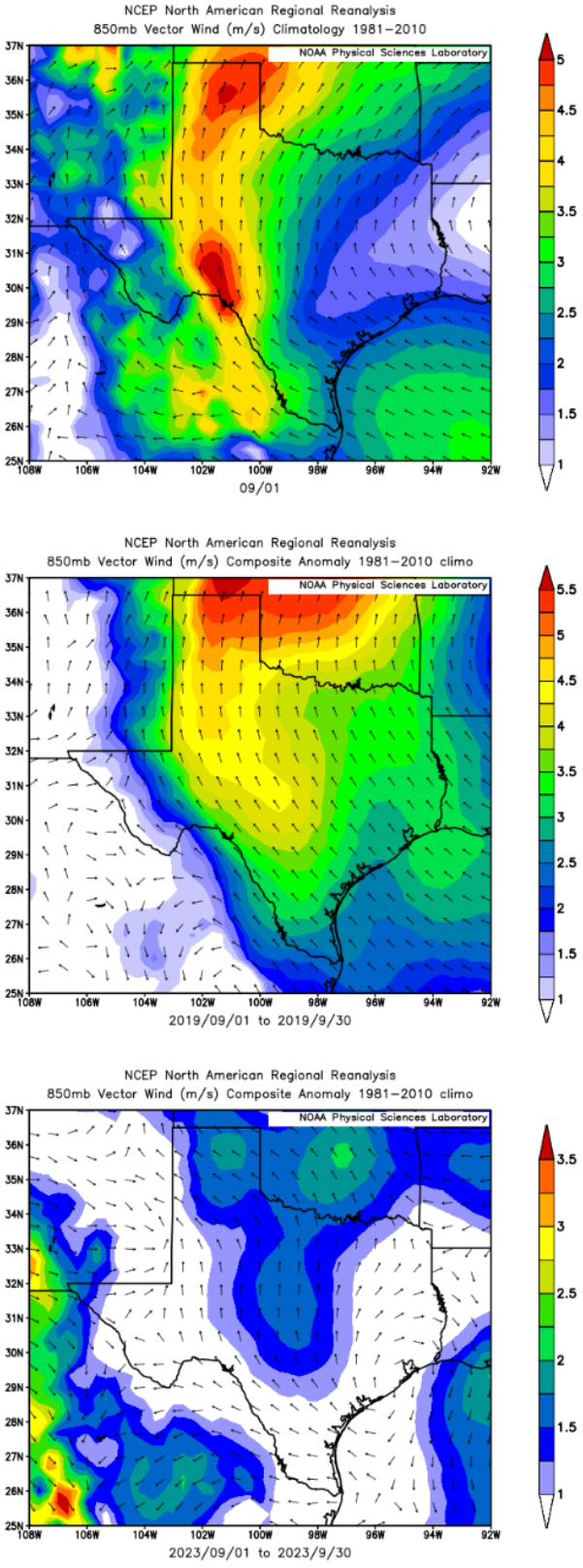

Figure 3-12. 850 mb wind vector climatology (top) and anomalies in 2019 (middle) and 2023 (bottom) focused on Texas.

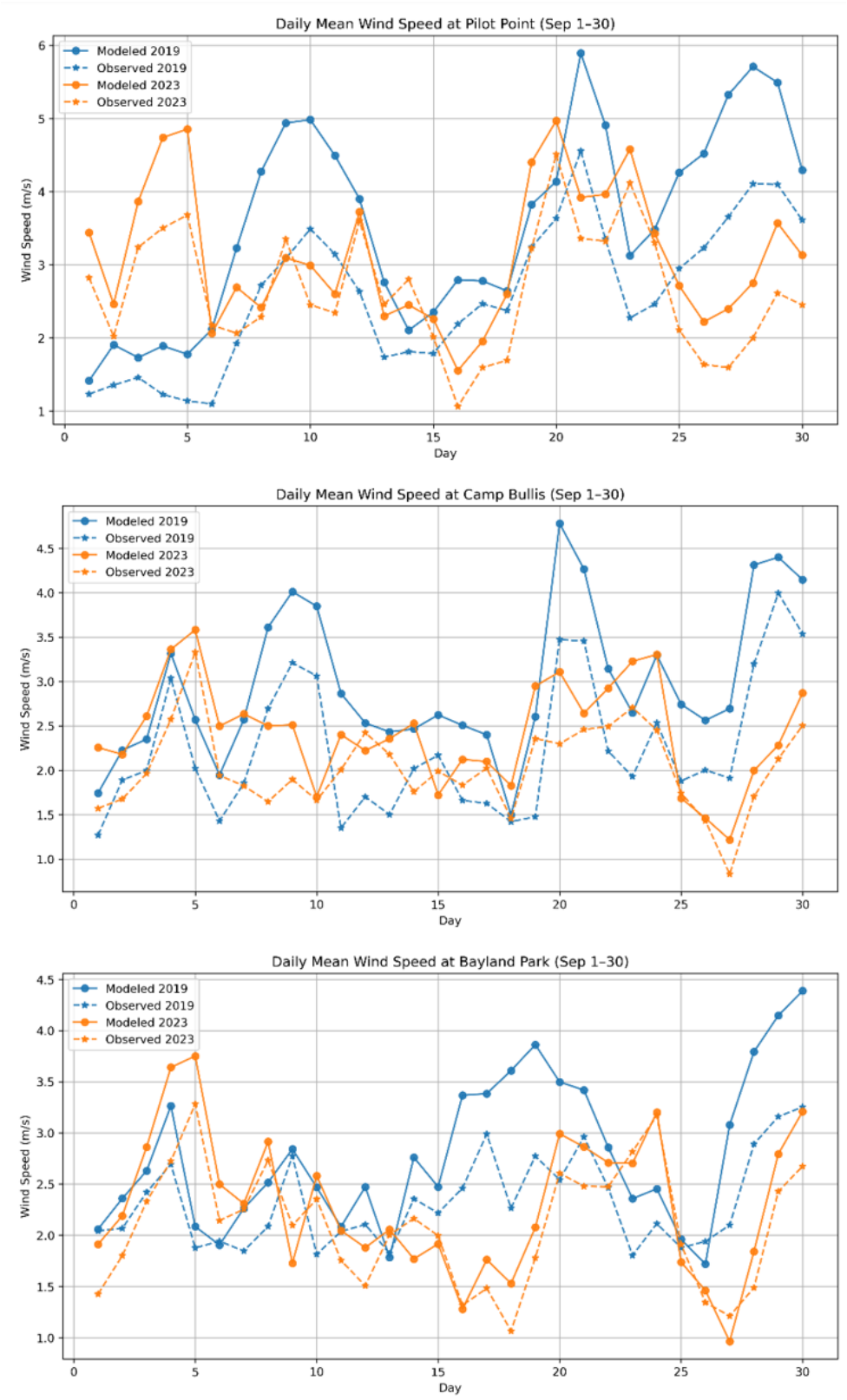

Figure 3-13. Simulated and observed daily mean surface wind speed at Dallas (top), San Antonio (middle), and Houston (bottom) during September 2019 and September 2023.

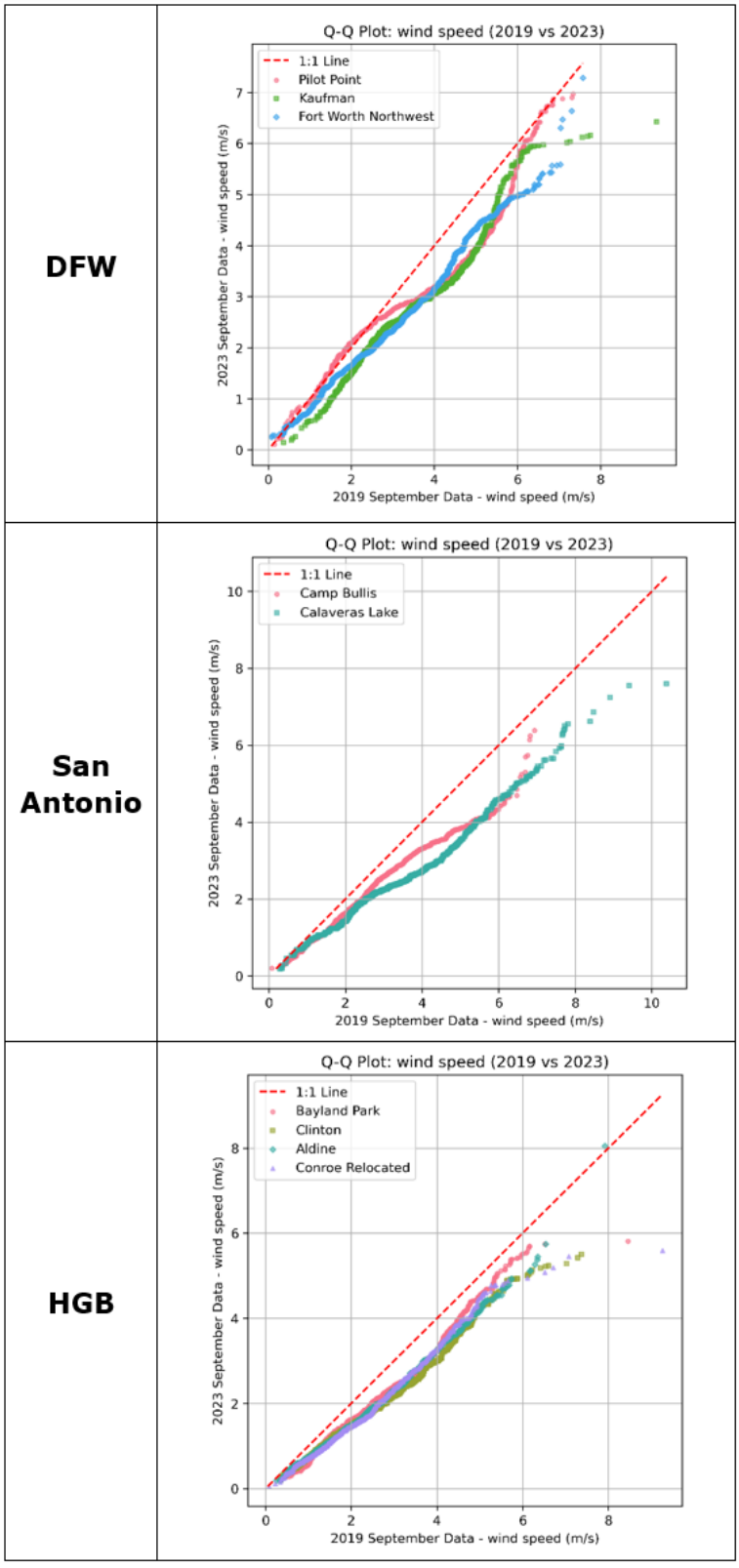

Figure 3-14. Q-Q plot showing intra-NAA comparisons of hourly surface wind speed in 2023 versus 2019 for DFW (top), San Antonio (middle) and HGB (bottom).

3.5 Planetary Boundary Layer Height

The climatology and anomalies for the planetary boundary layer (PBL) are presented in Figure 3-15. The PBL climatology shows a steep west to east gradient from deeper PBL in the west to shallower PBL over the Great Plains and toward the eastern U.S. The anomalies show that PBL had positive but similar anomalies for both 2019 and 2023 over Texas (note different scales among the two anomaly plots).[15] This is likely related to higher temperatures and lower cloud coverage in both years relative to climatology.

For the simulated PBL analysis, Ramboll considered the daily maximum PBL since peak vertical mixing coincides around the time of greatest photochemical activity (i.e. during midday hours). PBL observations were not added to these figures since measured PBL data were not available.

Figure 3-16 presents time series of simulated daily maximum PBL for September 2019 and 2023 at DFW, San Antonio, and HGB. Figure 3-17 compares 2023 versus 2019 simulated PBL heights for the three NAAs, along with an intra-NAA comparison. There is good consistency within each NAA but substantial variation between the three NAAs. The time series and Q-Q plots demonstrate rather variable results among the different NAAs, with no clear signals. Therefore, it is unclear how simulated PBL differences may have impacted ozone formation in 2019 compared to 2023.

[15] This analysis product is not available for the more recent climate period and was obtained from the NCEP North American Regional Reanalysis (NARR).

NCEP NARR Monthly/Seasonal Composites: NOAA Physical Sciences Laboratory

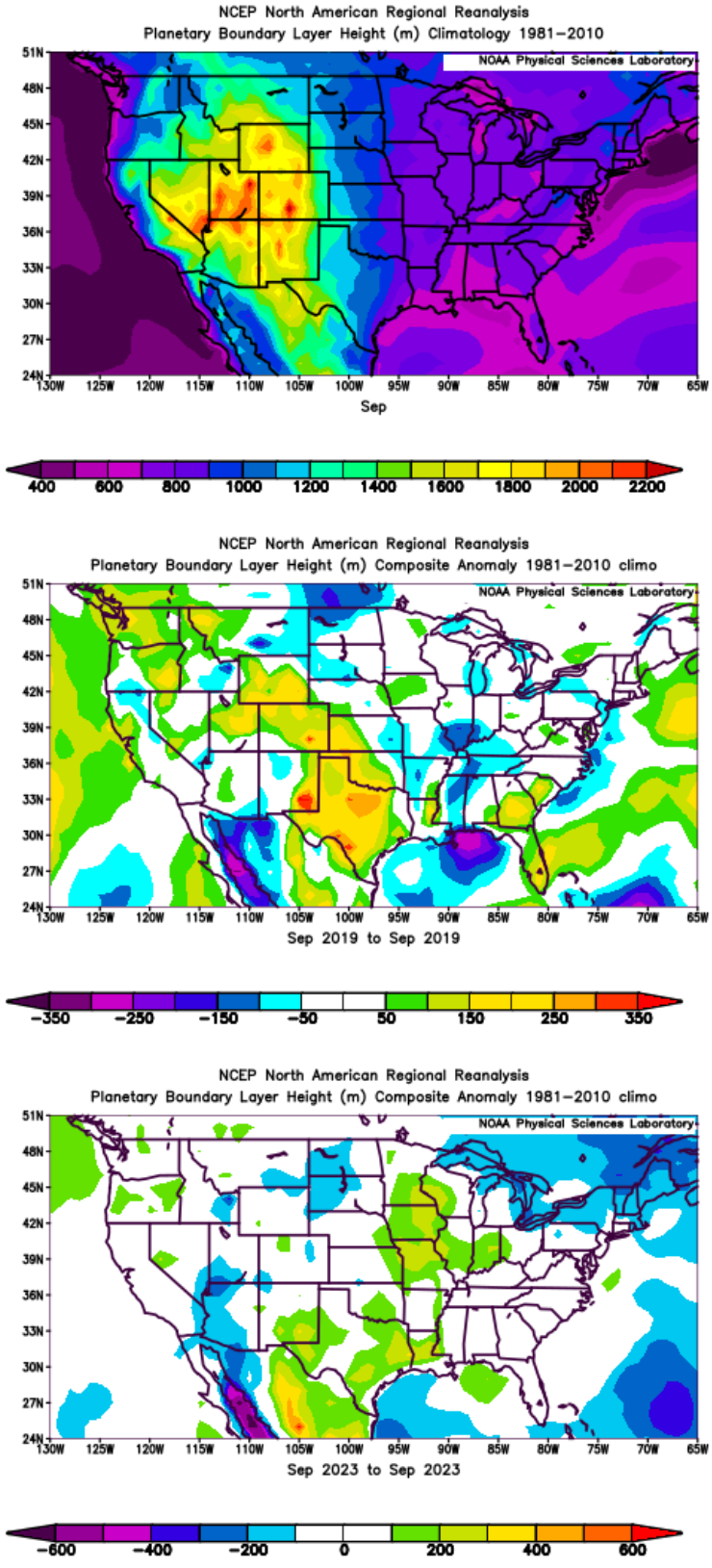

Figure 3-15. PBL climatology (top) and anomalies in 2019 (middle) and 2023 (bottom).

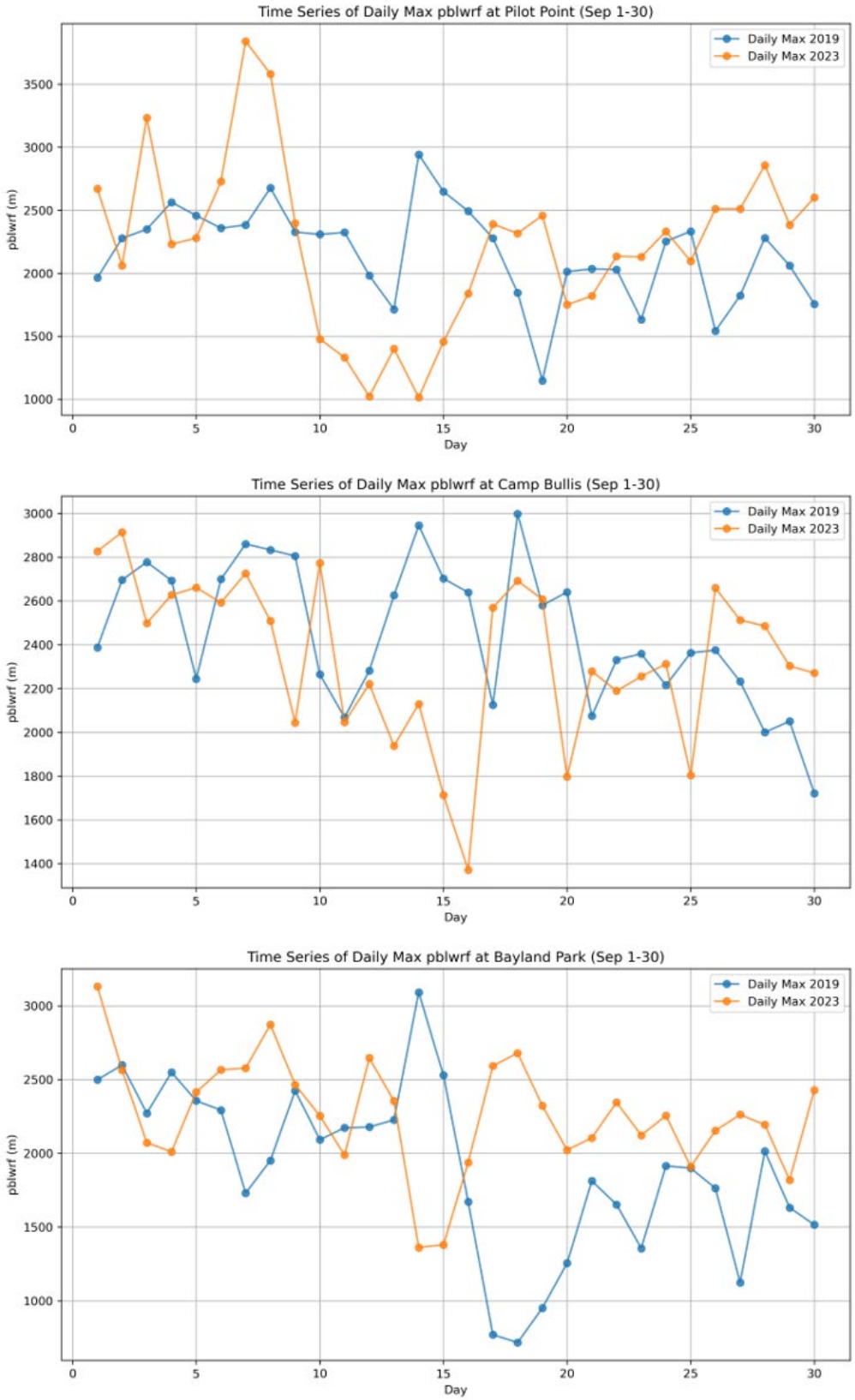

Figure 3-16. Simulated daily maximum PBL at Dallas (top), San Antonio (middle), and Houston (bottom) during September 2019 and September 2023.

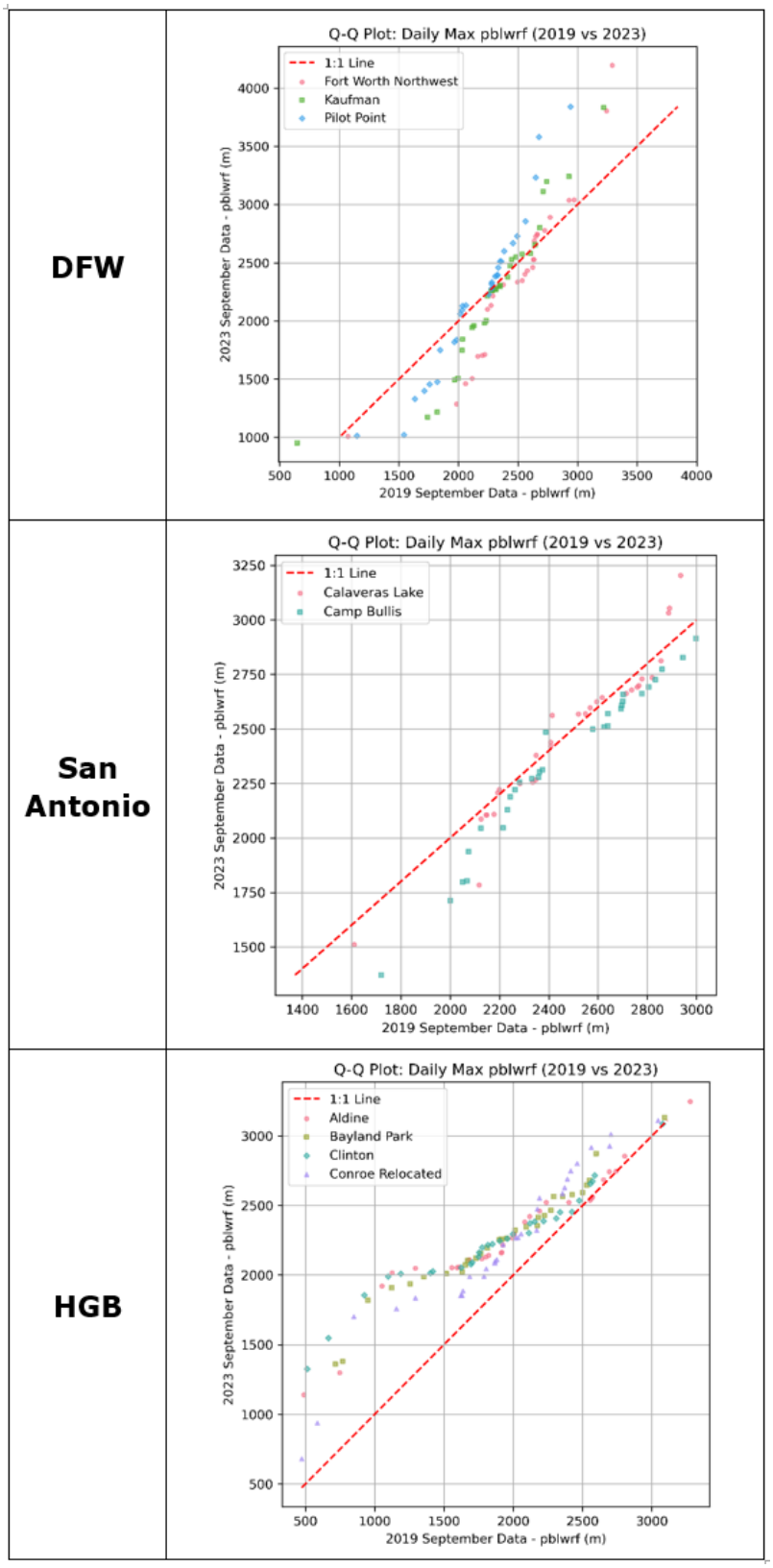

Figure 3-17. Q-Q plot showing intra-NAA comparisons of PBL in 2023 versus 2019 for DFW (top), San Antonio (middle) and HGB (bottom).

3.6 Meteorological Comparison Conclusions

Table 3-1 provides a summary of the meteorological analyses and Ramboll's assessment of potential impacts on ozone formation and/or CAMx ozone model performance.

Table 3-1. Summary of meteorological analysis.

Meteorological parameter	Summary Discussion	Potential Impacts
Temperature	The higher frequency of warmer days in 2023 likely contributed to higher ozone. (Section 3.1).	High
Modeled temperature performance	WRF daily maximum temperatures were slightly over-predicted, which may have had a minor impact on ozone. (Section 3.1).	Low
Solar radiation/cloud cover	More incoming solar radiation (i.e., sunny days) and more cloud free skies in 2023 likely contributed to higher ozone formation photochemistry. (Section 3.2).	Medium
Relative Humidity	The air over Texas and the Gulf of Mexico was generally drier in 2023, and drier conditions are associated with ozone episodes. (Section 3.3).	Low
Winds	More stagnant winds and less transport of cleaner air from the Gulf of Mexico in 2023 are likely to have contributed to higher ozone. Stagnation leads to the accumulation of ozone from local emissions sources with reduced dispersion. (Section 3.4).	High
Modeled wind speed performance	Systematic overprediction of WRF daily mean surface wind speeds could have led to more ventilation and lower accumulation of ozone resulting in a negative ozone bias in model results for all three CAMx simulations. (Section 3.4).	Medium
PBL	It is unclear from this analysis how PBL height may have impacted ozone formation in 2019 compared to 2023. (Section 3.5).	Unknown

4.0 CONCLUSIONS

Below are the key factors that explain the conditions that contributed to high ozone observed in Texas in September 2023 and why attainment demonstration modeling showed lower modeled ozone than observed.

Meteorological Factors

- Meteorological conditions in September 2023 were more conducive to ozone formation since that period was characterized by more stagnant winds and much less southerly flow (i.e., less transport of cleaner air from the Gulf of Mexico), as well as warmer temperatures and sunnier skies.
- Updating the CAMx model run using 2023 meteorology (instead of 2019 meteorology) but without updating emissions (i.e., Run 2 versus Run 1) greatly improved model performance at the controlling (i.e., highest ozone) monitors in the Houston, Dallas and San Antonio NAAs.
  - The improvement was characterized by a substantial reduction in the underestimates that were present for Run 1, particularly for high ozone days. Specifically, peak MDA8 ozone concentrations for Run 1 were underestimated by approximately 10 to 25 ppb across the three controlling NAA monitors, while Run 2 reduced the underestimate by approximately 7 to 10 ppb.
  - Anthropogenic and biogenic emission source contributions increased for Run 2 compared to Run 1 by approximately 5-15 ppb, and 1-5 ppb, respectively. This was likely due to increased local and regional ozone formation due to the warmer conditions and sunnier skies as well as more local accumulation due to reduced wind speeds.
- Model improvements were also seen at the additional monitors in Dallas and San Antonio, but not at the additional Houston monitors since for Run 1 the additional Houston monitors did not have substantial underestimates.
- WRF modeled wind speeds were higher than observed for both 2019 and 2023. This may be a contributing factor for the ozone under predictions for both meteorological years, due to increased ventilation and decreased ozone build-up of local emissions.

Emissions Factors

- The CAMx model run with updated 2023 emissions (i.e., as well as updated 2023 meteorology; Run 3) simulated lower total MDA8 ozone than Run 2 at all monitors in terms of September average MDA8 and peak MDA8.
- Run 3 exhibited degraded model performance compared to Run 2 at the controlling monitors in each NAA in terms of overall bias and replicating peak MDA8 ozone.

- The OSAT analysis revealed that the fire emissions source category resulted in the largest difference in ozone contributions between Run 2 and Run 3.
  - Fire contributions to monthly mean MDA8 ozone were approximately 5 ppb for Run 2 and 1 ppb for Run 3. Thus, the incorrect year fire emissions offset some underestimates in Run 2 (and Run 1). This is often termed "getting the right answer for the wrong reason".
- The OSAT analysis revealed that there were larger EGU ozone contributions in San Antonio than in Houston or Dallas, and the EGU ozone concentrations were more responsive to the Run 3 EGU emissions updates in San Antonio than in Houston or Dallas.

Summary and Recommended Future Work

The primary reason that the attainment demonstration modeling projected lower modeled ozone than observed was that it was based on 2019 meteorology, which was less conducive to ozone formation than 2023 meteorology. Updating the modeling to 2023 meteorology and updating 2023 emissions resulted in higher modeled ozone concentrations and improved model performance compared to the attainment demonstration modeling but still underestimated peak ozone. Ramboll recommends further study to investigate additional reasons for the ongoing underestimates. Furthermore, WRF meteorological model performance for wind speeds should be investigated, since the analyses suggest wind speeds are overestimated and could lead to underestimates of ozone due to increased ventilation of local emissions.

5.0 REFERENCES

Ramboll 2024. User's Guide – Comprehensive Air Quality Model with Extensions Version 7.31. Available at www.camx.com.

Skamarock, W.C., et al., 2019. A Description of the Advanced Research WRF Model Version 4. NCAR Technical Note TN-556+STR, Mesoscale and Microscale Meteorology Laboratory, National Center for Atmospheric Research, Boulder, CO (March). https://opensky.ucar.edu/islandora/object/opensky:2898.

Emery, C., Liu, Z., Russell, A. G., Odman, M. T., Yarwood, G., & Kumar, N. (2017). Recommendations on statistics and benchmarks to assess photochemical model performance. *Journal of the Air & Waste Management Association*, *67*(5), 582–598. https://doi.org/10.1080/10962247.2016.1265027

Appendix A – Ozone Evaluation at Additional Monitors

Appendix A CAMx Evaluation at Additional Monitors

1.1 Intra-NAA Analyses

To evaluate potential intra-NAA variations, additional monitors were selected based on discussion with TCEQ, these monitors are listed in Table 1 with spatial characteristics.

Table 1. Intra-NAA monitors selected for the analysis.

Nonattainment Area	Additional Selected Monitor(s)	AQS Site ID	Latitude	Longitude	CAMx 4km grid I	CAMx 4km grid J
HGB	Clinton	482011035	29.733726	-95.257593	124	112
HGB	Aldine	482010024	29.901036	-95.326137	122	117
HGB	Conroe Relocated	483390078	30.350302	-95.425128	119	129
DFW	Kaufman	482570005	32.564968	-96.317687	97	191
DFW	Fort Worth Northwest	484391002	32.80581	-97.356529	73	197
San Antonio	Calaveras Lake	480290059	29.275381	-98.311692	49	99

Figure 1. CAMx Model Performance for Houston: Clinton.

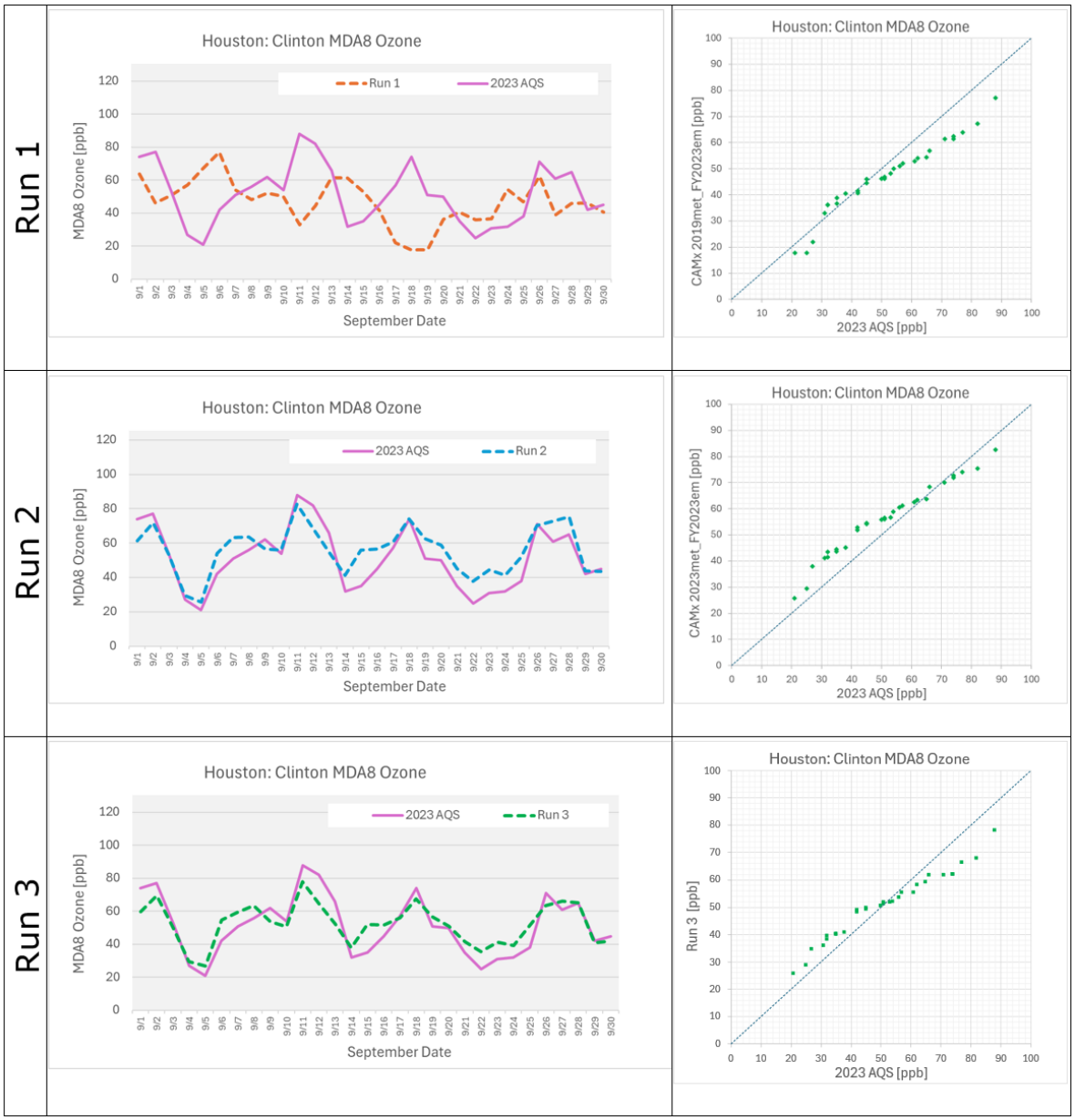

Table 2. CAMx model MDA8 ozone performances statistics for Houston: Clinton.

Metric	2023 AQS	Run 1	Run 2	Run 3
September Mean MDA8 [ppb]	51.4	46.8	55.9	52.4
September 4th high MDA8 [ppb]	74.0	62.4	72.8	66.1
NMB MDA8 %	-	-8.9	8.8	2.0
NME MDA8 %	-	37.4	16.0	14.5
R	-	-0.20	0.88	0.89

Figure 2. CAMx OSAT results for Houston: Clinton.

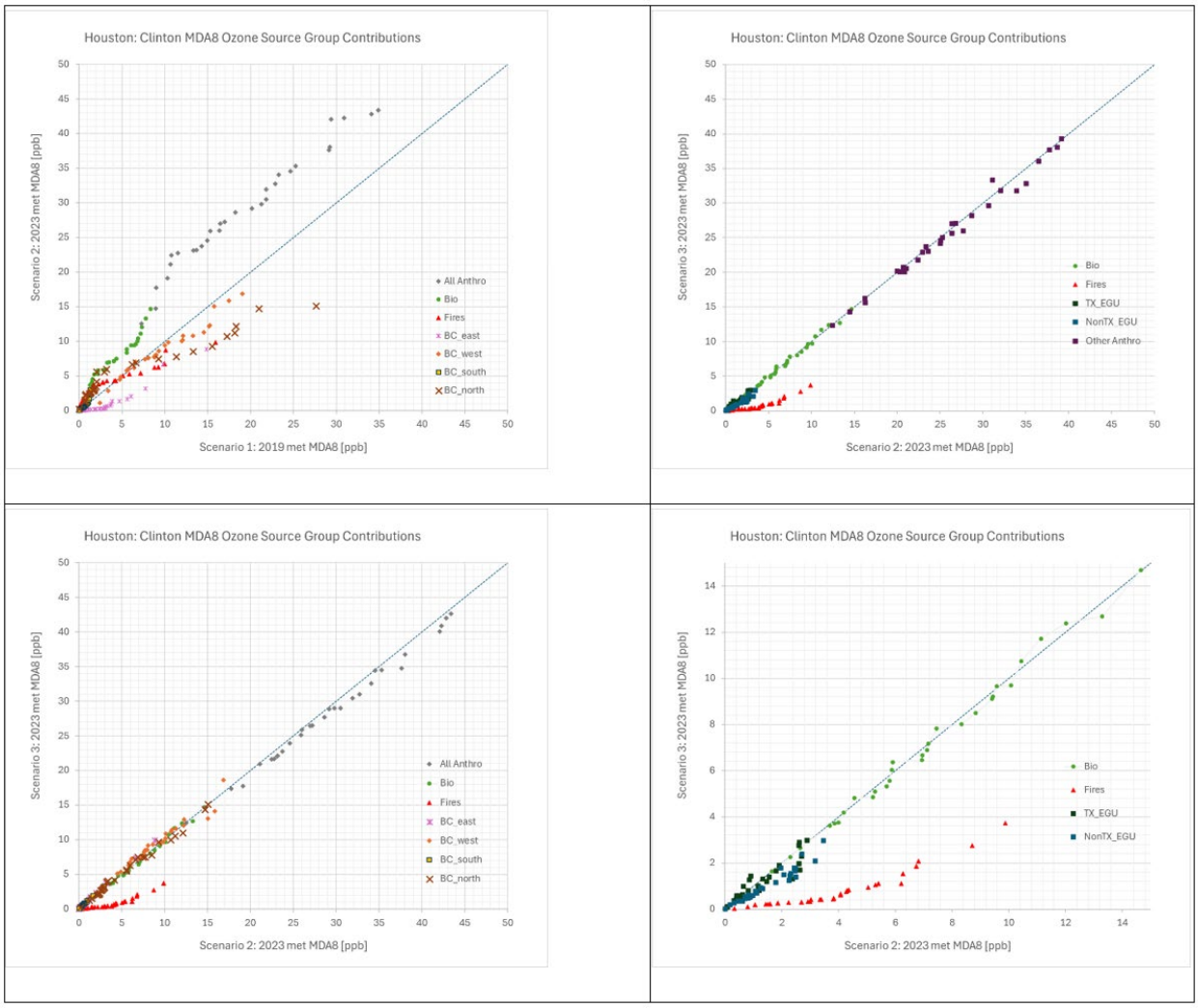

Figure 3. CAMx model performance for Houston: Aldine.

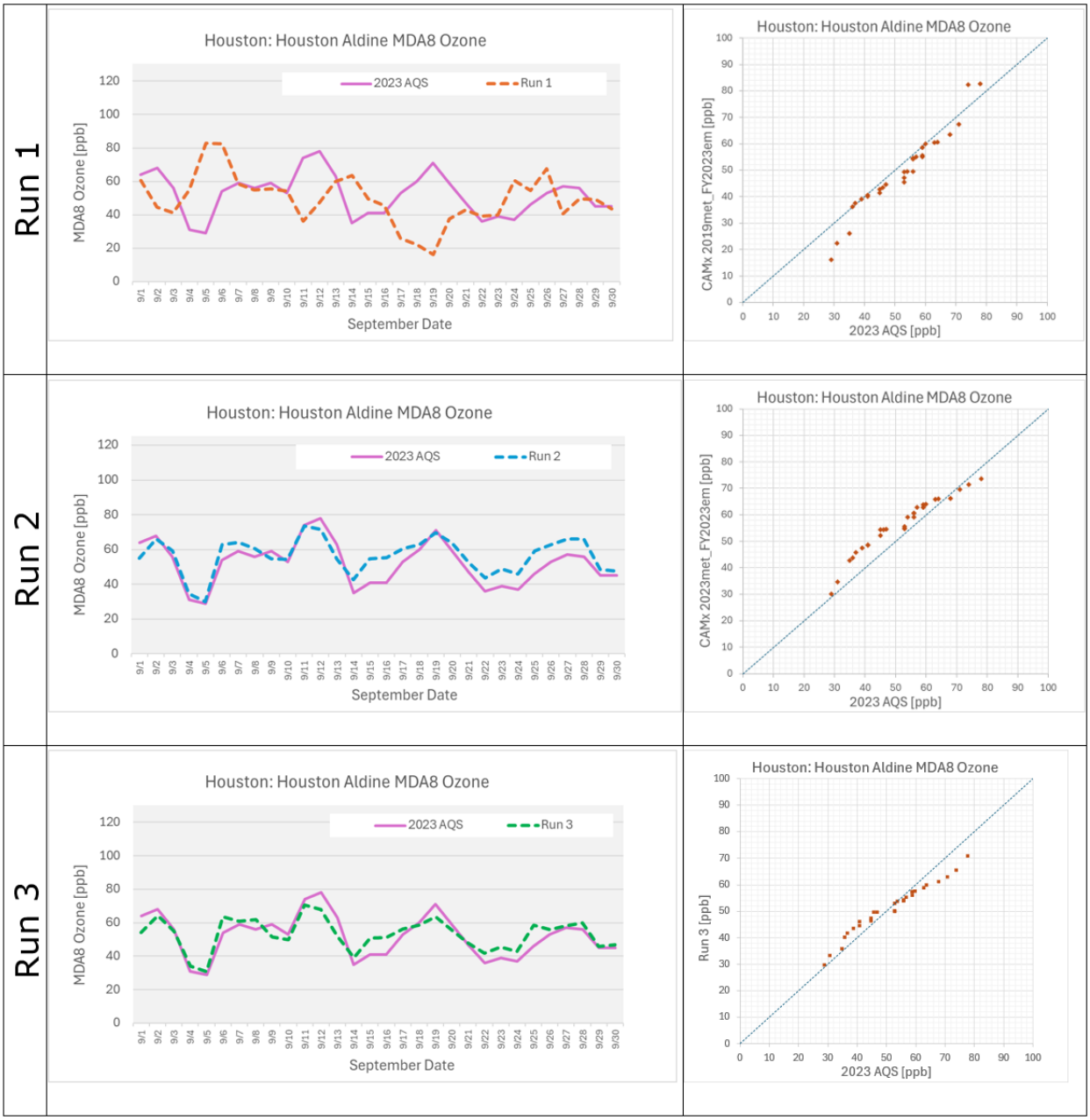

Table 3. CAMx model MDA8 ozone performance statistics for Houston Aldine.

Metric	2023 AQS	Run 1	Run 2	Run 3
September Mean MDA8 [ppb]	52.2	49.4	56.4	53.2
September 4th high MDA8 [ppb]	68.0	63.4	66.1	63.7
NMB MDA8 %	-	-5.4	8.1	2.0
NME MDA8 %	-	31.4	12.2	9.8
R	-	-0.35	0.87	0.88

Figure 4. CAMx OSAT results for Houston: Aldine.

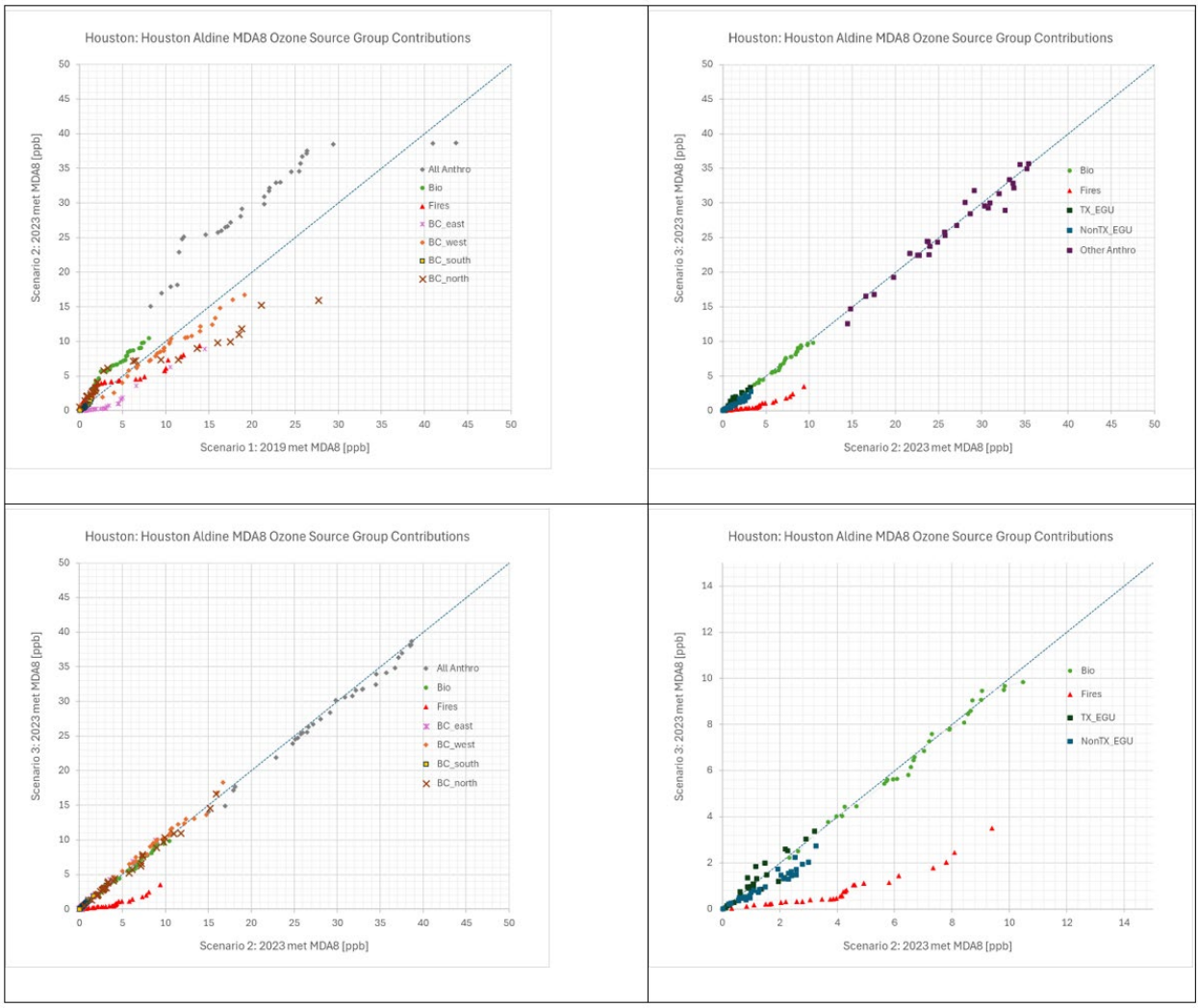

Figure 5. CAMx model performance for Houston: Conroe Relocated.

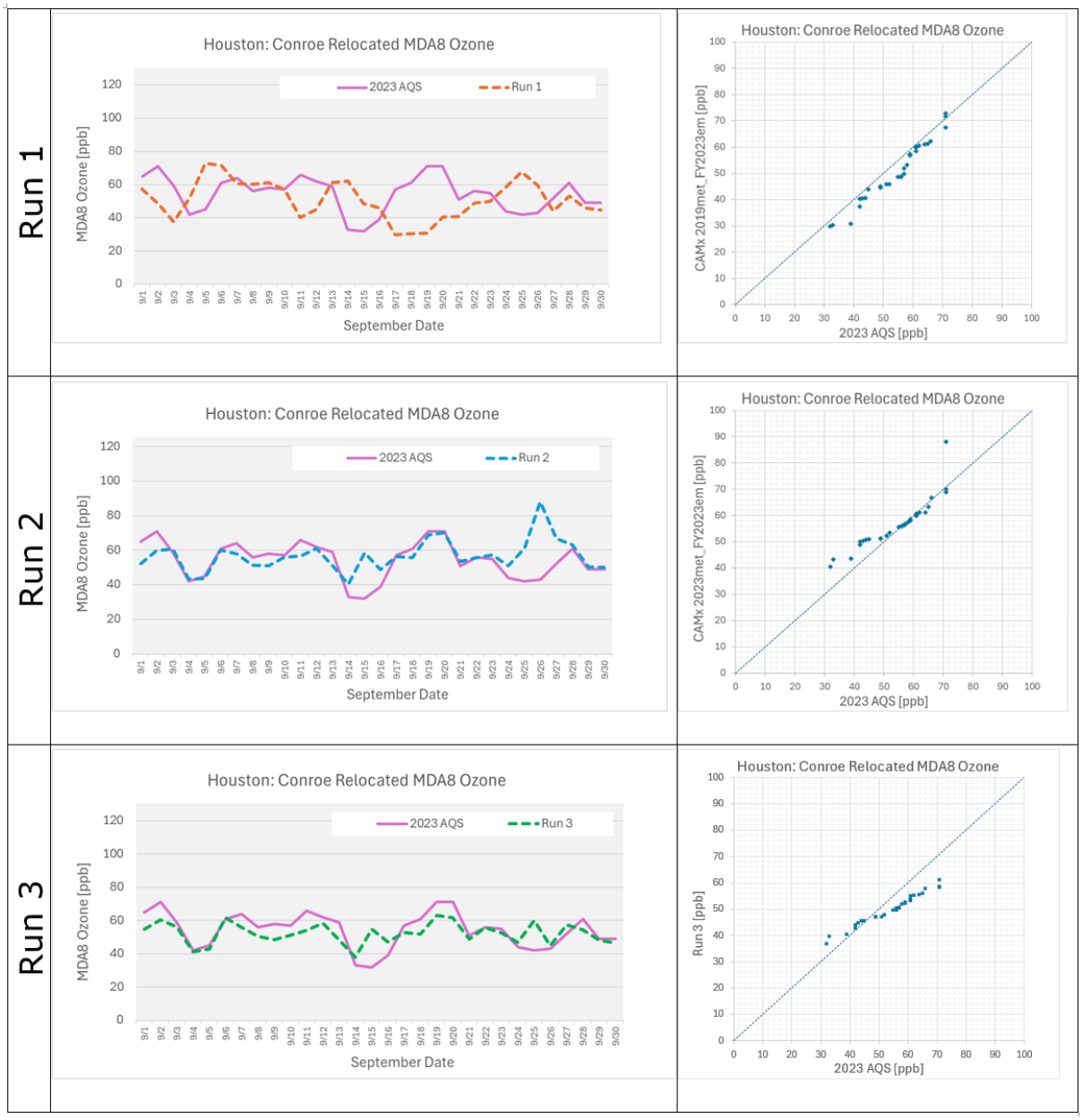

Table 4. CAMx model MDA8 ozone performance statistics for Houston: Conroe Relocated.

Metric	2023 AQS	Run 1	Run 2	Run 3
September Mean MDA8 [ppb]	54.4	50.9	56.7	52.3
September 4th high MDA8 [ppb]	66.0	62.3	66.8	60.3
NMB MDA8 %	-	-6.5	4.3	-3.8
NME MDA8 %	-	27.0	13.2	11.8
R	-	-0.32	0.32	0.66

Figure 6. CAMx OSAT results at the Houston Conroe Relocated monitor.

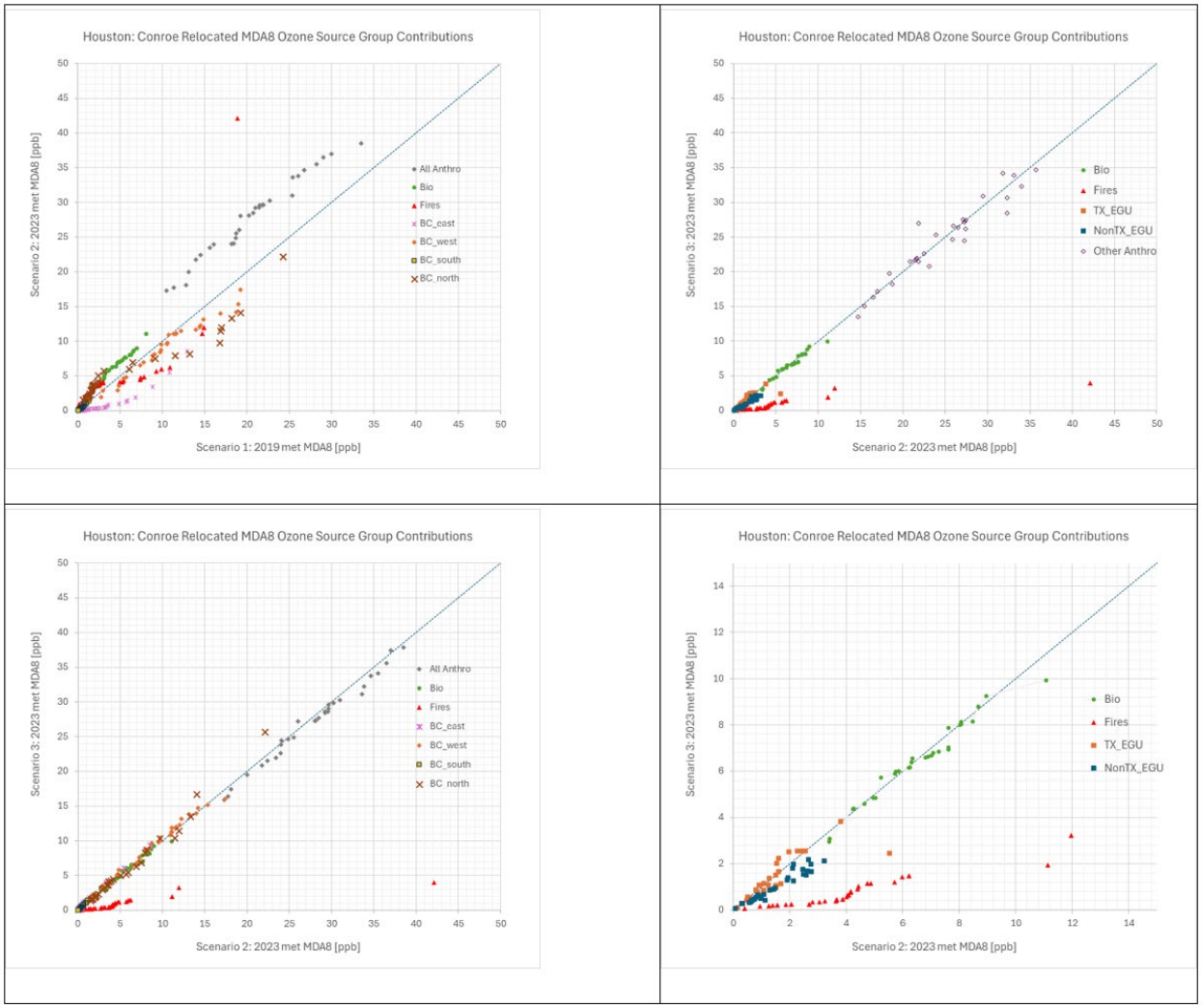

Figure 7. CAMx Model Performance for Dallas: Kaufman.

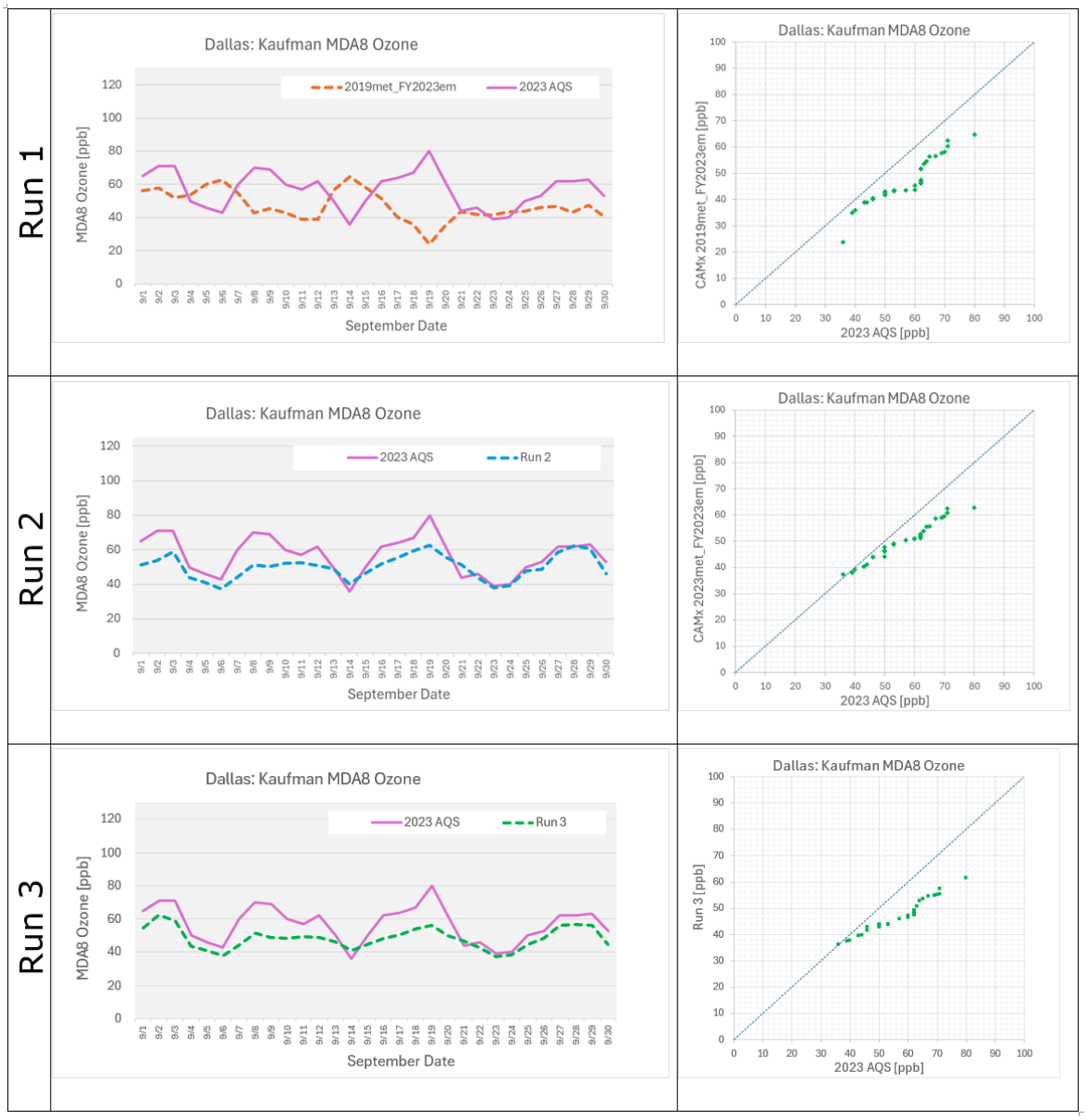

Table 5. CAMx model MDA8 ozone performance statistics for Dallas: Kaufman.

Metric	2023 AQS	Run 1	Run 2	Run 3
September Mean MDA8 [ppb]	56.9	47.0	50.2	48.4
September 4th high MDA8 [ppb]	70.0	58.2	59.4	56.2
NMB MDA8 %	-	-17.3	-11.8	-15.0
NME MDA8 %	-	27.6	13.2	15.9
R	-	-0.40	0.81	0.86

Figure 8. CAMx OSAT results for Dallas: Kaufman.

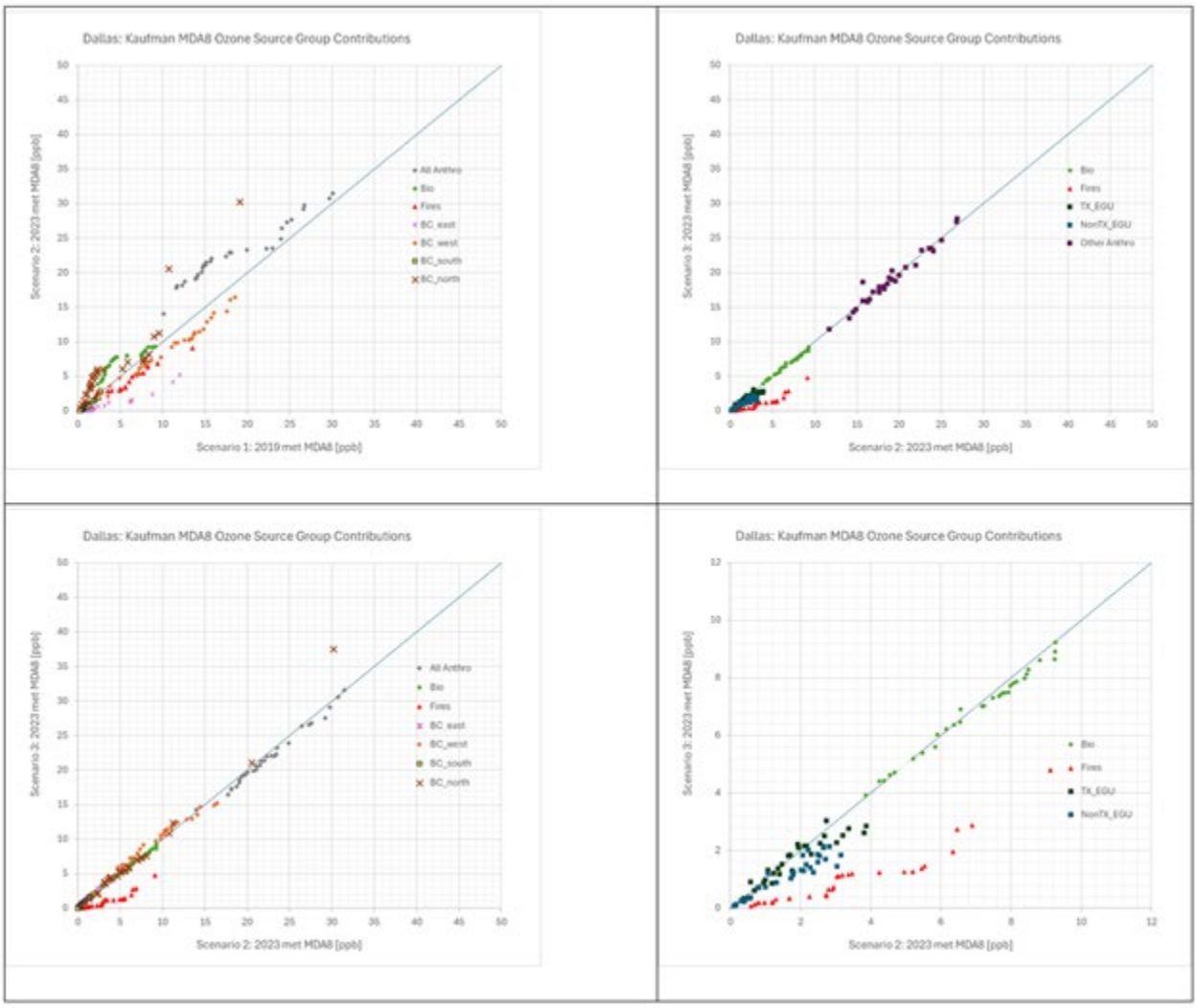

Figure 9. CAMx model performance for Dallas: Fort Worth Northwest.

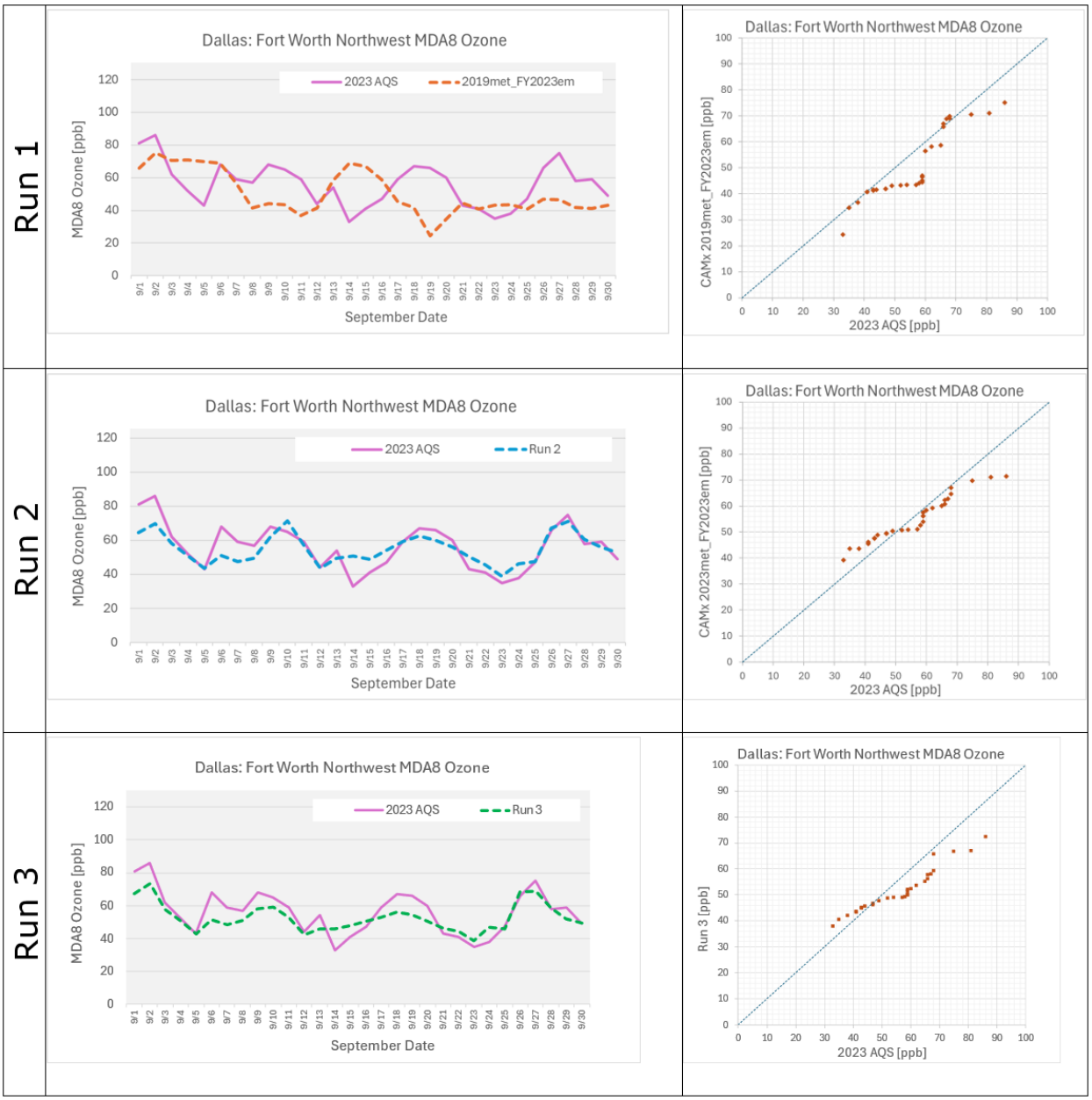

Table 6. CAMx model MDA8 ozone performance statistics for Dallas: Fort Worth Northwest.

Metric	2023 AQS	Run 1	Run 2	Run 3
September Mean MDA8 [ppb]	56.1	50.6	54.9	52.6
September 4th high MDA8 [ppb]	68.0	69.9	67.1	67.4
NMB MDA8 %	-	-9.8	-2.0	-6.2
NME MDA8 %	-	27.5	10.6	11.6
R	-	0.07	0.83	0.88

Figure 10. CAMx OSAT results for Dallas: Fort Worth Northwest.

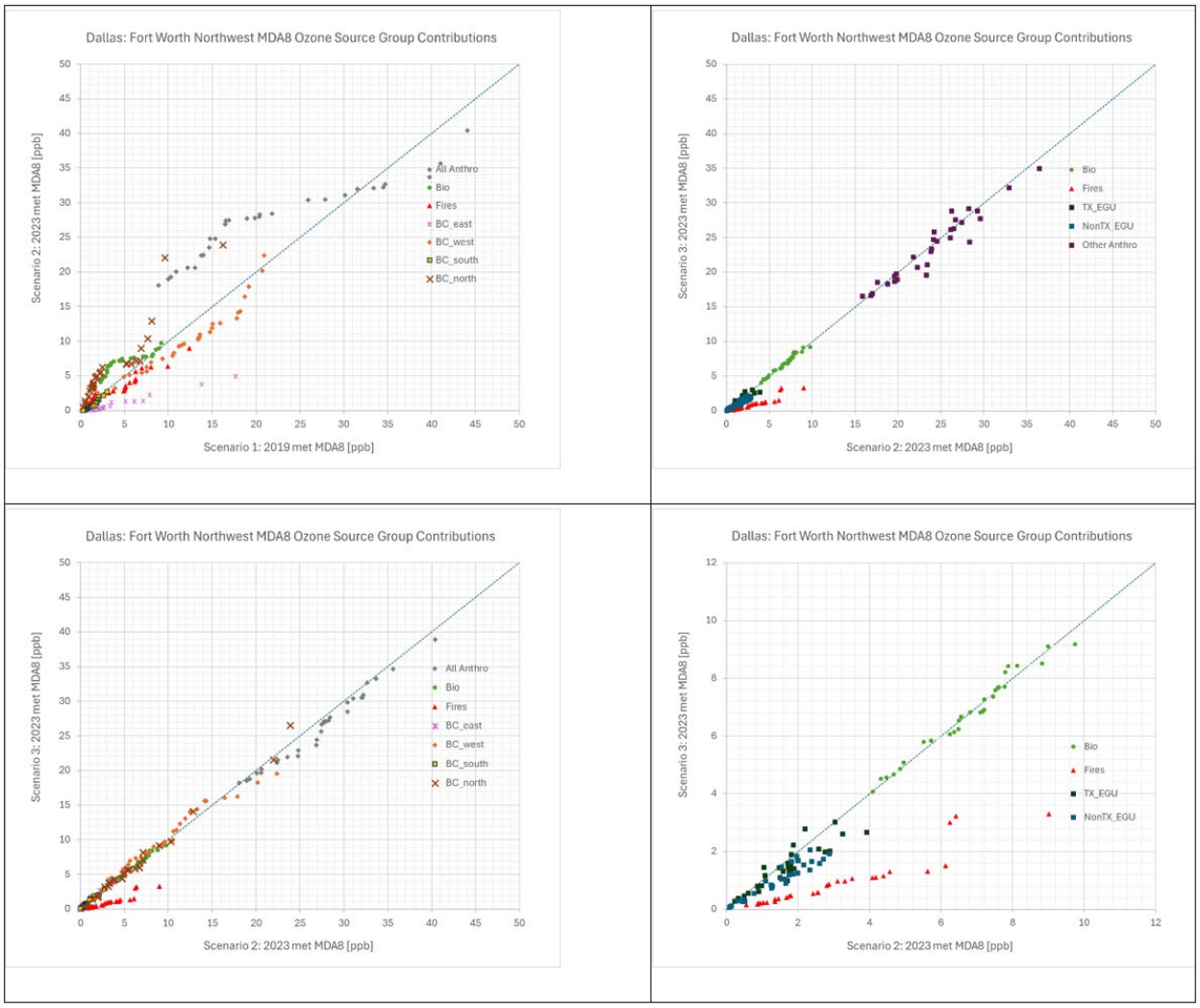

Figure 11. CAMx Model Performance for San Antonio: Calaveras Lake.

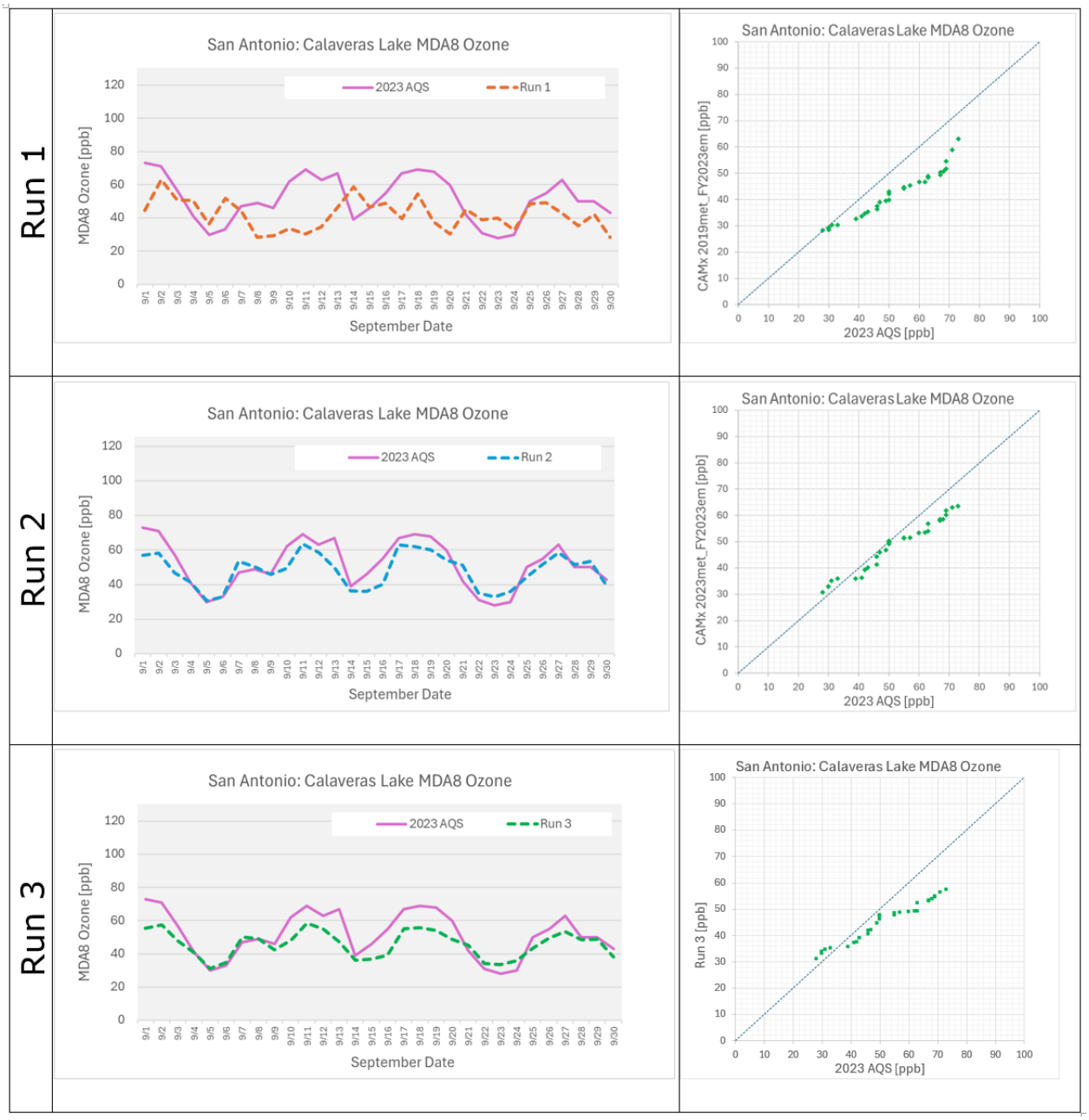

Table 7. CAMx model MDA8 ozone performance statistics for San Antonio: Calaveras Lake.

Metric	2023 AQS	Run 1	Run 2	Run 3
September Mean MDA8 [ppb]	51.8	42.1	48.1	45.8
September 4th high MDA8 [ppb]	69.0	51.7	60.2	55.4
NMB MDA8 %	-	-18.7	-7.1	-11.5
NME MDA8 %	-	29.1	12.0	14.7
R	-	0.11	0.87	0.90

Figure 12. CAMx OSAT results for San Antonio: Calaveras Lake.